Anticipatory smooth eye movements scale with the probability of visual motion: role of target speed and acceleration

Vanessa Carneiro Morita, David Souto, Guillaume S Masson, Anna Montagnini

Anticipatory smooth eye movements scale with the probability of visual motion: role of target speed and acceleration

Vanessa Carneiro Morita[1], David Souto[2], Guillaume S. Masson[1] and Anna Montagnini[*,1]

1 Institut de Neurosciences de la Timone, CNRS & Aix-Marseille Université, Marseille, France

2 School of Psychology and Vision Sciences, University of Leicester, Leicester, United Kingdom.

* Corresponding author

Acknowledgements: This work was funded by the *Agence Nationale de la Recherche* (ANR-PREDICTEYE 18-CE37--0019 to GSM, AM) and the *Fondation pour la Recherche Médicale* (Equipe FRM 2018 to GSM) and by Aix-Marseille Université (PhD Doctoral extension funding to VCM). We would like to thank Mr Alexis Ulian for helping in the data collection of the Experiment 2A as part of his Master internship.

Abstract

Sensory-motor systems are able to extract statistical regularities in dynamic environments, allowing them to generate quicker responses and anticipatory behavior oriented towards expected events. Anticipatory smooth eye movements (aSEM) have been observed in primates when the temporal and kinematic properties of a forthcoming visual moving target are fully or partially predictable. However, the precise nature of the internal model of target kinematics which drives aSEM remains largely unknown, as well as its interaction with environmental predictability. In this study we investigated whether and how the probability of target speed or acceleration is taken into account for driving aSEM. We recorded eye movements in healthy human volunteers while they tracked a small visual target with either constant, accelerating or decelerating speed, keeping the direction fixed. Across experimental blocks, we manipulated the probability of the presented target motion properties, with either 100% probability of occurrence of one kinematic condition (fully-predictable sessions), or a mixture with different proportions of two conditions (mixture sessions). We show that aSEM are robustly modulated by the target kinematic properties. With constant-velocity targets, aSEM velocity scales linearly with target velocity across the blocked sessions, and it follows overall a probability-weighted average in the mixture sessions. Predictable target acceleration/deceleration does also have an influence on aSEM, but with more variability across participants. Finally, we show that the latency and eye acceleration at the initiation of visually-guided pursuit do also scale, overall, with the probability of target motion. This scaling is consistent with Bayesian integration of sensory and predictive information.

Introduction

Pursuit eye movements allow us to maintain steady on the retinas the image of a moving object of interest. To do so, tracking eye movements rely heavily on the visual estimate of the moving target's speed and direction (Carl & Gellman, 1987; Lisberger & Westbrook, 1985; Tychsen & Lisberger, 1986). When the target moves at constant speed in the visual field, the eyes start accelerating in the same direction as the target motion after a relatively short visuomotor latency (~100-130 ms in humans (Carl & Gellman, 1987)). In the optimal speed range for human pursuit (i.e. below 20-30°/s), the eyes typically reach a steady state velocity close to the target's velocity within ~300 ms from visual motion onset. Steady-state smooth tracking, in close coordination with the so-called "catch-up saccades" can maintain a relatively good alignment between the fovea and the target position over time (Carl & Gellman, 1987; J.-J. Orban De Xivry & Lefèvre, 2007). Despite the fact that natural objects rarely move with a constant velocity, only a few studies have investigated smooth tracking for constantly accelerating or decelerating target motion. Those studies reported that humans are able to track visible targets with smoothly-varying speed (e.g. Bennett & Benguigui, 2013; Kreyenmeier et al., 2022) but pursuit of constantly accelerating targets, seems to be limited in terms of accuracy. Similar to perceptual discrimination judgments, tracking eye movements carry poor discriminative power about visual acceleration compared to visual speed (e.g., Watamaniuk & Heinen, 2003). These previous works were thus mainly concerned about whether, and with which accuracy, the primate visual motion system can

extract and represent motion acceleration for moving targets (Lisberger & Movshon, 1999).

Our dynamic environment and the stimuli motion properties are often, at least in part, predictable, because either the motion is produced by our own body (e.g., Gauthier et al., 1988; Landelle et al., 2016), or it can be inferred from general prior knowledge, past experience or perceptual cues (Kowler et al., 2019). When the moving target's velocity changes in a periodic way (e.g., sinusoidal motion), after a few cycles our gaze can dynamically adapt to the predictable motion and align to the target with virtually no lag (Kowler & Steinman, 1979a). Importantly, motion predictability allows not only to smoothly pursue a moving target with a reduced lag but also to anticipate its motion onset, or its reappearance after a transient occlusion (e.g. Dodge et al., 1930; for a review, see Kowler et al., 2019 and Fukushima et al., 2013). It is commonly assumed that anticipatory smooth eye movements (aSEM) that are initiated before target motion onset would contribute to quickly reduce the retinal position and velocity errors (i.e. the difference between the eye's and the target's position or velocity respectively) during the early phase of motion tracking (e.g. Kao & Morrow, 1994). Target motion predictability can be manipulated across different time scales (e.g. across or within trials in a standard visuomotor experiment) and aSEM were described in a range of conditions of repetitive (or weakly varying among trials) target motion conditions along simple trajectories and with constant speed (e.g., among many others, in Barnes & Asselman, 1991; Heinen et al., 2005; Kowler & Steinman, 1979b). However, much less is known about aSEM for accelerating and decelerating targets. One of the few

studies that report aSEM for accelerating targets showed that during the transient disappearance of the target (*blank* paradigm) amplitude of predictive smooth eye movements scales with target acceleration (Bennett & Barnes, 2006).

Our group, and others have previously shown that aSEM amplitude is proportional to the probability of a given target motion direction in a direction-biased task (Damasse et al., 2018; Montagnini et al., 2010; Santos & Kowler, 2017). Expectation for a given target speed also modulates aSEM: anticipatory eye velocity increases with speed predictability, in a random versus fully predictable speed design (e.g., Heinen et al., 2005; Jarrett & Barnes, 2002; Kao & Morrow, 1994). However, we still do not know whether other kinematic parameters, such as the acceleration profile can be taken into account when predicting time-varying target speed or direction. Moreover, whereas it has been reported that aSEM velocity increases linearly with the probability of target direction, the functional dependence of anticipatory eye velocity upon the probability of target velocity, or of its acceleration, was not investigated so far, to our knowledge, or only to a very limited degree (Bennett, Orban De Xivry, et al., 2010).

It is well known that tracking eye movements synchronize almost perfectly with target motion kinematics during for instance sinusoidal (Barnes & Asselman, 1991), or circular (Orban De Xivry et al., 2008) trajectories. However, such synchronization develops over seconds and it is not obvious to tease apart the respective contribution of position, velocity and acceleration signals (Lisberger &

Movshon, 1999). So far, target acceleration does seem to be suboptimally integrated in predictive pursuit, even on a shorter time scale, such as during the transient disappearance of a moving object. For instance, when an accelerating target is occluded after a short presentation (~ 200 ms), eye velocity during the blanking period reduces, and its predictive reacceleration prior to the target reappearance is not influenced by the target acceleration (Bennett et al., 2007). However, if the target visibility window before the occlusion is long enough (> 500 ms), eye velocity reduces during the blanking period, but recovers in an acceleration-scaled manner prior to the target reappearance (Bennett, Orban De Xivry, et al., 2010). Moreover, in a task where participants are asked to track a target and to predict the target position after a given period of time, or to predict when the target is going to reach a certain position, both after the target is occluded, target acceleration is not appropriately taken into account for the responses (Bennett & Benguigui, 2013; Kreyenmeier et al., 2022). In principle, anticipating the motion trajectory of a forthcoming accelerating target, by estimating the rate of change of its velocity, would help the eye to more rapidly and more accurately reach the target's velocity and position during visually-guided tracking movement. Conversely, anticipation would be suboptimal if it were only determined by the initial target velocity or by its temporal average across a limited visible motion epoch disregarding its rate of change, resulting in larger position/velocity errors at the end of the open-loop tracking phase. To disentangle these alternatives, we aimed at better understanding how target motion kinematics shape aSEM.

Finally, visually-guided pursuit initiation can provide a more constrained framework to tease apart sensory and predictive computations (Bogadhi et al., 2013; Orban De Xivry et al., 2013) and identify the contribution of different kinematic cues. Since the pioneering work of Kao and Morrow (1994), very sparse empirical efforts have been put into building an integrated framework of how predictive information coordinates anticipatory and visually-guided phases of tracking eye movements. On the other hand, in the past decades optimal motor control theory and the Bayesian framework (e.g. Körding & Wolpert, 2004) have gained interest in the study of human movements. A few recent studies, including ours, have applied such computational framework, sometimes in the form of the Kalman filter approach, to oculomotor control (e.g., Bogadhi et al., 2013; Darlington et al., 2018; Deravet et al., 2018; Orban De Xivry et al., 2013). Overall, these studies have shown that inferential integration models can account for the role of target motion predictability on both the anticipatory (strongly driven by the Prior) and the visually-guided phases (driven by a reliability-weighted combination of the Prior and sensory information) of tracking eye movements. More recently, Darlington et al (2018) provided the first evidence that pursuit-related neuronal preparatory activity in macaque frontal eye fields (FEF) can provide the neural correlate of the prior information which is integrated with the sensory evidence to drive ocular tracking. Therefore, the second objective of the current study was to precisely estimate the dependency of the early visually-guided pursuit phase across the different speed/acceleration probability conditions, in order to probe the general validity of the inferential integration model.

To summarize, in the present study, we first tested aSEM behavior for targets moving in a fully predictable direction but with ramp-like motions of different speeds and accelerations. We manipulated the probability of each kinematic condition across blocks. We showed that the probability of target motion speed controls aSEM similarly to the probability of motion direction, with a linear dependence of anticipatory velocity upon the target speed probability. We also showed that aSEM can be triggered by predictable accelerating/decelerating targets, in a way that accounts for the expected target's velocity change and for its probability.

Second, we measured how eye velocity during the early portion of the visually-guided phase of tracking is shaped by the target motion properties in interaction with their predictability. We focused in particular on the latency and early acceleration of visually-guided pursuit and, despite the lack of complete homogeneity in the results, our data suggest that pursuit initiation is overall coherent with the Bayesian integration hypothesis.

Methods

Participants

Twenty-one healthy adult volunteers signed an informed consent to participate in the experiments presented in this study. The experimental protocol was approved by the Ethics Committee *Comité de Protection des Personnes OUEST III* (CPP reference: PredictEye-2018-A02608-47), in full respect of the Helsinki

declaration guidelines. Three of the authors (AM, GM, DS) participated in Experiment 1 (n = 3), two of the authors (AM, VCM) participated in Experiment 2A (n = 13) and one of the authors (VCM) participated in the Experiment 2B (n = 5). In Experiment 1, anticipatory eye movements and initial pursuit were recorded with high precision by using the scleral search coil technique (Robinson, 1963) in a small participant sample. The core finding of this experiment motivated the Experiments 2A,B on a larger sample of participants using a less invasive technique (video eye tracking) that confirmed the main results. A preliminary version of the results from Experiment 1 was presented previously at the VSS conference (Souto et al., 2008).

Stimuli and procedure

In all experiments, participants were instructed to visually track a moving target by smoothly pursuing it with their gaze, as accurately as they could, while their eye movements were recorded.

Experiment 1

The detailed methods are described elsewhere (Wallace et al. 2005). Briefly, a PC running the REX package controlled both stimulus presentation and data acquisition. Stimuli were generated with an SGI Fuel workstation and back-projected onto a large translucent screen (80° x 60°, viewing distance: 1m) using a Barco 908s video-projector (1280”, 1024 pixels at 76 Hz). Oculomotor recordings were collected using the scleral search coil technique (Collewijn et al. 1975). This experiment probed aSEM in different speed probability contexts (**Figure 1a**). Each trial started with a fixation point, located at the centre of the screen for a

random duration between 300 and 450 ms. If the participant fixed accurately (i.e. within a 2°-side, square electronic window) during the last 200 ms, the fixation target was extinguished and followed by a fixed-duration, 300 ms gap with nothing on the screen. At the end of the gap period, the target (a white, gaussian-windowed circle, 0.2 ° std, maximum luminance 45 cd/m^2) appeared at the centre of the screen and started moving horizontally, to the right, for a fixed period of 500 ms. The target speed was either 5.5 °/s (LS) or 16.5 °/s (HS). In each experimental block, a different target speed-bias condition defined the proportion of trials at high speed (P(HS) = 0, 0.1, 0.25, 0.5, 0.75, 0.9 and 1, respectively). The complementary proportion of trials had a low speed target motion (P(LS) = 1-P(HS)). Participants completed 500 trials per block, except for the P(HS) = 0 and P(HS) = 1 conditions where only 250 trials were completed. One or two blocks were completed in a day, with the constraint of not exceeding a total of one hour of duration.

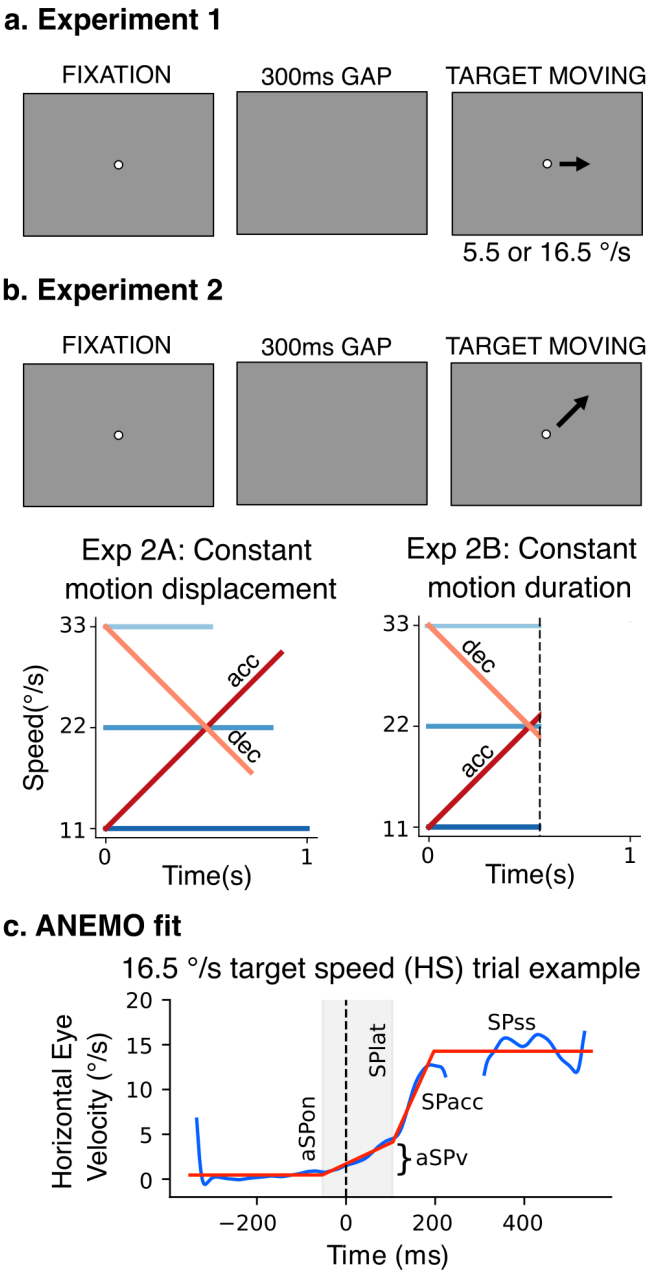

Figure 1. Experimental designs. Each trial started with a fixation point at the centre of the screen for a random period, followed by a gap of 300 ms. The target then appeared at the centre of the screen and started moving. **(a). Experiment 1.** The target moved to the right at one of the two constant speeds (5.5 or 16.5 °/s). The probability of a high-speed (P(HS), v = 16.5 °/s) vs a low-speed (P(LS) = 1-P(HS), v = 5.5 °/s) trial was varied between experimental blocks with 7 different values of P(HS) (0, 0.1, 0.25, 0.5, 0.75, 0.9, 1). **(b). Experiment 2.** The target always moved in a fixed direction, chosen between one of the four diagonals (counterbalanced between participants). We displayed three different constant target speeds (v11, v22, v33 of 11, 22 and 33 °/s, respectively), one accelerating (vacc,

acc = 22 °/s^2) and one decelerating (vdec, acc = -22 °/s^2) speed profiles. In a first version of the experiment (Exp 2A), conditions were designed with a constant target displacement, while in a second version of the experiment (Exp 2B) the time duration of the target motion was kept constant at 600 ms (black dashed line). **(c) Template analysis of eye velocity profiles.** The bottom panel shows an example of the eye velocity trace (blue curve) and of the ANEMO model fit (red curve, Pasturel et al., 2018[1]) in an individual trial. From this model were extracted the onset of the anticipatory phase (aSPon), its maximum velocity (aSPv), the latency of the visually guided pursuit (SPlat) and its open-loop acceleration (SPacc), and the steady state of the eye velocity (SPss). The model fit to this data was similar to the Experiment 1, except the steady state that was not fitted.

Experiment 2

Experiment 2A

Stimuli were presented using the Psychtoolbox (Brainard, 1997) package for MATLAB. The Display++ monitor (CRS) with a refresh rate of 120 Hz, was placed at 57 cm distance in front of the participant. Eye movements were recorded using an Eyelink1000, an infrared video-based eye tracker (SR Research). This experiment probed aSEM with different target constant and varying speed conditions, while manipulating the probability of each condition. With respect to Experiment 1, a larger pool of participants was tested with a different set of speed values and a smaller set of speed probabilities. Because several studies showed a strong anisotropy for saccadic and smooth pursuit eye movements across the two-dimensional plane (e.g., Grasse & Lisberger, 1992; Ke et al., 2013; Rottach et al., 1996; Takeichi et al., 2003), we decided to test the generalizability of the results found for Experiment 1 beyond the horizontal direction. Therefore, in Experiment 2

[1] The ANEMO analysis pipeline is available at: https://github.com/invibe/ANEMO/tree/master/ANEMO

the target moved along one of the four diagonal directions, counterbalanced between participants.

Figure 1b shows the experimental design. Each trial started with a fixation dot in the center of the screen for a random interval between 300 ms and 600 ms. This fixation period was followed by a fixed gap window of 300 ms. At the end of the gap window, the target appeared at the center of the screen and started moving in one of the four diagonal directions (always the same for one participant) with different target kinematics conditions: the target speed was either constant (v11, v22, and v33; 11, 22, and 33 °/s respectively), accelerating (vacc; starting from 11 °/s, a = 22 °/s^2), or decelerating (vdec - starting from 33 °/s, a = -22 °/s^2). In Experiment 2A, target motion duration was adapted to the target kinematic properties in order to achieve a similar spatial displacement on the screen across conditions: in practice target movement lasted 1, 0.82, and 0.52 s for v11, v22 and v33, respectively, 0.87 s for vacc, and 0.72 s for vdec.

Participants first completed 5 blocks of 100 trials with a single target kinematics condition (v11, v22, v33, vacc, vdec, “fully-predictable” blocks, presented in randomized order across participants). Notice that these conditions can be considered as a probability of 1 for each kinematic value and allow us to estimate anticipatory and visually-driven pursuit initiation under these different fully-predictable target kinematics. Next, the probability of the different target kinematics was manipulated across blocks of 200 trials each (“mixture blocks”). For constant speed blocks, we used v11 and v33, with P(v33) being equal to either 0.3

or 0.7 and P(v11) = 1-P(v33). The two probability levels were presented in random order across participants. For the time-varying speed blocks, P(vdec) could be either of 0.3 or 0.7 (P(vacc) = 1-P(vdec). Again, these two probability conditions were randomly interleaved.

Experiment 2B

Having different motion durations across conditions might have introduced some confounds affecting the resulting anticipatory behavior. First, the estimate of the acceleration of a visual target can be impaired if the target is presented too shortly (Bennett, De Xivry, et al., 2010; Bennett et al., 2007). Second, if anticipatory behavior relies on the estimate of mean target velocity, rather than on its accelerating dynamics (Brouwer et al., 2002; Gottsdanker et al., 1961; Schmerler, 1976), then the duration of the motion epoch might influence the mean velocity estimate for targets with time-varying speed. Therefore, we ran an additional control experiment (Exp 2B) with the same design as Exp 2A but with two differences. First, target motion duration was held constant (600ms), resulting in different target end positions across conditions. Second, we collected the 5 blocks of a single, fully-predictable, target kinematics and the 2 blocks of probability-mixture for the time-varying target kinematics, but not the 2 blocks of probability-mixture for the constant target speeds, considering that Experiment 1 already follows a fixed duration design.

Eye-tracker recordings and preprocessing

For Experiment 1, the analog voltage measure collected with the scleral coil technique and reflecting the right-eye rotation was low-pass filtered (DC-130 Hz) and digitized with 16-bit resolution at 1000 samples per second (to obtain the eye's horizontal and vertical position). For Experiment 2A and 2B, the right-eye horizontal and vertical position was recorded with an infrared video-based eye tracker, EyeLink 1000 (SR Research), at 1 kHz.

For all sets of recorded eye movements, position data was converted in an ASCII format. After conversion, the ANEMO package (Pasturel et al., 2018) and custom-made python scripts were used to pre-process the data. Position data was low-pass filtered (acausal second-order Butterworth low-pass filters, 30 Hz cut-off), numerically differentiated to get the eye velocity in degrees per second and then de-saccaded using ANEMO's implementations. Trials with more than 70% of missing data points in the +/- 100 ms window around the target onset, or with more than 60% of missing data points overall, were automatically excluded from the pre-processing pipeline. ANEMO was used to fit a piecewise linear model to individual trials' eye velocity in order to extract the relevant oculomotor parameters (see **Figure 1c** for an illustration of the model fitting and parameters). Relevant model-fit parameters were the temporal onset of the anticipatory phase (aSPon), the maximum velocity of the anticipatory phase (aSPv), the latency of the visually guided pursuit (SPlat) and its initial acceleration (SPacc). For Experiment 1, an estimate of the pursuit steady-state velocity (SPss) was also extracted from the

model (**Figure 1a**, bottom panel), but not further analyzed in this article. However, when inspecting the ANEMO fit to the Experiment 1' data, we noticed that for low-speed trials, the model was not adapted to the eye velocity dynamics. In short, for low-speed trials occurring in blocks with high probability for high speed trials, the eye velocity at the visually guided pursuit initiation was consistently above the target speed, and sometimes it even underwent a small "dip" before a reacceleration (the latter phenomenon also occurred for high-speed trials). Since the ANEMO model constrains the fit of visually-guided eye velocity between the anticipatory value and the steady state of the eye velocity, it could not fit this pattern of eye velocity data and in the end it did not allow for a reliable estimation of the latency and initial pursuit acceleration. In this case, we decided to use a more local and less constrained fitting model, aiming at estimating two regression lines around the end of the anticipatory phase and the open-loop phase of the visually-guided pursuit in order to extract the latency and initial pursuit acceleration. More specifically, we fitted two regression lines in two different time windows of 50 ms. The first regression line could be fitted in any 50ms time window between [70, 120] ms and [100, 150] ms. The best regression was chosen based on Pearson's R between the real eye velocity values and the ones predicted by the regression. The second regression line could be fitted in any 50ms time window between [130, 180] ms and [150, 200] ms, with the constraint that the first and second regression lines' windows did not overlap. Again the best regression was chosen based on Pearson's R. The intersection of the two regression lines was considered as the latency, and the slope of the second regression line was considered as the initial acceleration of

the visually guided pursuit. We visually inspected the fitted regression lines and the estimated latency across trials. Note that even though this method improved consistently the latency detection, we still had a considerable number of trials in which we could not determine the intersection between the two regression lines in a reasonable interval (between 80 and 180 ms after the target onset), because the eye velocity did not change enough and the regression lines were almost parallel: each participant had between 21 and 44% of the trials without a reliable estimation of the latency.

Eye velocity traces and model fits were visually inspected to exclude the remaining aberrant trials and those with extremely poor fits. Overall, 5% of the trials were excluded on average for Experiment 1 (median: 2.5 %, max: 10 %), 11% for Experiment 2A (median: 11 %, max: 20 %), and 6 % for Experiment 2B (median: 6 %, max: 9 %).

Data analysis

In all experiments, when analyzing the effects of the probability bias, the first 50 trials of each block were excluded from analysis. The probability bias is likely to have reached an asymptote well before 50 trials, as suggested by work on history effects (e.g. Maus et al., 2015; Pasturel et al., 2020), allowing us to focus on average values and not their rate of change.

Linear Mixed Effects Models (*nlme* package for R) were used to evaluate the effects of the target kinematics (different constant speed and acceleration conditions) and of the probability context on the oculomotor parameters extracted

from the ANEMO's fit to oculomotor recordings. Because not including a true random effect can increase the false positive rate (Barr et al., 2013), participants were treated as a random effect and all fixed effects were allowed to vary with it. Since this approach usually leads to models that don't converge because of the high number of parameters and the correlations between them, when needed, we used the *buildmer* package for R (Voeten, 2020) to find the maximal model (i.e., the model including the most of variables) which still converges for each dependent variable. After finding the models, we fitted the data and result tables were exported with the *stargazer* package for R (Hlavac, 2022).

For Experiment 1, the models included only the speed probability as a fixed effect for the oculomotor anticipation parameters (aSPon, aSPv). We chose to use the probability of the highest speed, P(HS), as the independent variable in the model 1:

$$(1)\ \ anticipatory\ parameter \sim 1 + P(HS) + (1 + P(HS) \mid participant)$$

and for the visually guided parameters (SPlat, SPacc) we added an interaction with the target kinematics, *Tk*, in model 2:

$$(2)\ \ visually\ guided\ parameter \sim 1 + P(HS) * Tk + (1 + P(HS) + Tk \mid participant)$$

The variable before the ~ symbol is the dependent variable, and the variables after it are the independent variables (also called fixed effects). The 1 corresponds to the model intercept. For the variables within the parentheses, each one before the | symbol is allowed to vary for each level of the variable after it (also called random

effect). In other words, for each participant, the model will return a different best-fit value for the intercept and the slope of the dependence upon probability. Since the models 1 and 2 were simple and converged in all cases, we did not do a model selection. For the analysis of the probability-mixtures of Experiment 2 (v11 vs v33, vacc vs vdec), we also added the axis (horizontal/vertical) as an interaction factor with the probability, given that the target moved along one of the diagonals. For the vacc vs vdec condition mixture analysis, we included an interaction with the experiment (2A/2B). The final models, as well as the statistics tables are presented in the supplementary material.

To check for the effect of the constant-speed, accelerating and decelerating targets on the parameters extracted from the model fit in Experiments 2A and 2B, the "fully-predictable" conditions were tested for the effects of target kinematics (*Tk*). Again, we included the direction axis (*axis*) as an interaction factor to determine whether there were significant differences between the horizontal and vertical components of the eye velocity. Also, in order to test for differences between Experiments 2A and 2B, we included a variable indicating to which experiment each trial belonged (*exp*). Therefore, the LMM initial formulation was:

$$(3)\ parameter \sim 1 + Tk * axis * exp + (1 + Tk + axis + exp | participant)$$

The *Tk* variable indicates the target motion condition between v11, v22, v33, vacc or vdec. Note that, because we did not have a strong hypothesis about the parametric dependence of oculomotor anticipatory parameters upon target

acceleration or deceleration, we defined the target kinematics as a categorical variable.

In the analysis of the equivalent target speed, we calculated for each participant the regression :

*(4) aSPv = slope*Tk + intercept*

In this case, Tk included V11, V22, and V33. We then used the inverse operation to find the equivalent constant speed that would have elicited the observed aSPv for Vacc and Vdec:

(5) Predicted target speed = (aSPv - intercept)/slope

We finally estimated the (2D) joint-distributions of the predicted target speeds and anticipatory eye velocity (Figure 6) using the *seaborn* package for python (v0.12.2), with the default parameters for the kernel density estimation (Scott method with equal weights for all inputs).

Results

Effects of target speed probability on anticipatory Smooth Eye Movements

Using a state-of-the-art eye movement recording technique (scleral search coil), we first investigated the effects of target speed probability upon anticipatory smooth eye movements. In Experiment 1, three participants had to smoothly pursue a target which moved rightward along the horizontal axis with two different

possible speeds (HS and LS) randomly interleaved across trials but with a given probability (P(HS) and P(LS)=1-P(HS)) within a block. **Figure 2a** shows the trial-averaged eye velocity curves for one participant, sorted by probability and target speed conditions. Each probability condition is represented by one shade of blue (lighter shades corresponding to higher probabilities of high-speed). The two different target speed profiles are illustrated by the horizontal dotted lines, and time zero corresponds to target motion onset. Participants were able to track the two target motions with high accuracy, as shown by the convergence of eye velocity to the proper target speed during steady-state pursuit. Since target motion direction was always rightward, we observed a strong anticipatory response for all speed probability conditions, as evidenced by the non-zero eye velocity at the usual pursuit latency in humans (~100 ms). However these anticipatory responses were also modulated by the speed probability. We analyzed such modulation by considering the relationship between amplitude of anticipatory responses and P(HS), the probability of the highest speed (16.5 °/s). As illustrated in **Figure 2a**, higher values of P(HS) (lighter shades of blue) drove stronger anticipatory pursuit, regardless of the target speed (16.5 ou 5.5 °/s). **Figure 2b** plots the relationship between mean anticipatory eye velocity (aSPv) and P(HS), for the 3 participants. The gray curves are the linear relationships estimated from the Linear Mixed Effects Model (LMM). We found a clear linear dependency of anticipatory response and probability of target speed, in the direction of target motion. The LMM statistical analysis (with P(HS) as a fixed effect) shows that aSPv significantly increased with higher probability (P(HS) effect: beta = 3.14, 95% C.I. = (2.87, 3.41), $p < .001$).

Overall, anticipatory responses were stronger by ~100 %, rising from 2.5 to 5.5 °/s when P(HS) increased from 0 to 1, but also started earlier. We found a significant decrease of aSPon as P(HS) increased (**Figure 2c**, P(HS) effect: beta = -15.90, 95% C.I. = (-20.81, -10.99), $p < .001$). Across the 3 participants, anticipation for P(HS) = 0 started at ~ -83 ms, decreasing up to ~ -101 ms before target motion onset, for P(HS) = 1.

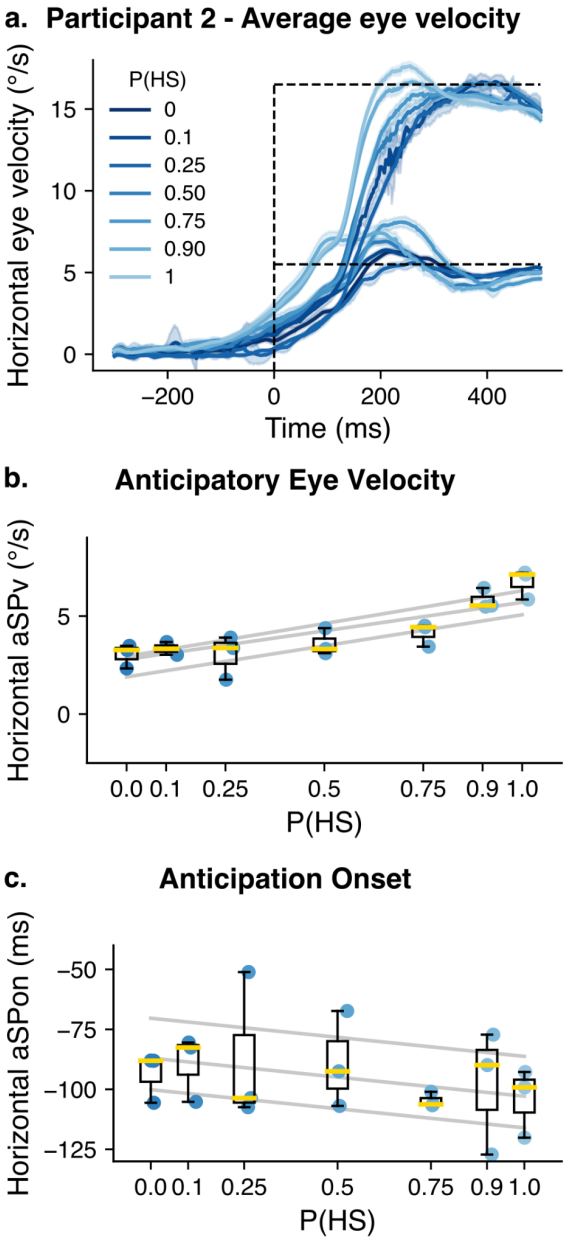

Figure 2. Experiment 1: Dependence of anticipatory eye velocity upon target speed probability. **(a)**. Average eye velocity as a function of time (+/- 95% confidence interval) for one representative participant. Trials are grouped by probability of the higher speed (HS). Each shade of blue corresponds to one probability condition (lighter shades for higher probabilities of HS). The time zero corresponds to the target onset, and the dashed lines indicate the two possible target speeds. **(b)**. Anticipatory eye velocity for the group of participants. Each box plot (median in yellow, box limits corresponding to the 25% and 75% quartiles, and whiskers corresponding to 1.5*IQR (interquartile range)) corresponds to one probability condition. The gray lines show the linear mixed model fit

for each participant. **(c)**. Anticipation onset for the group. Again, each box plot corresponds to one probability condition and the gray lines indicate the LMM fitted to each participant.

In the second Experiment (Exp 2A), our first objective was to replicate the speed-probability dependency of anticipatory pursuit on a larger group of 13 participants, with a less invasive eye tracking technique. We used different speeds (11, 22 and 33˚/s) and a reduced set of probability conditions (0, 0.3, 0.7 and 1). Now using an oblique target motion direction, our second objective was to generalize this speed probability dependency across the visual field, by having the target moving along the 4 oblique directions (**Figure 1b**). We first report the effects of target speed probability observed when varying across blocks P(v33) and therefore P(v11) = 1-P(v33) within (v11,v33) mixes. **Figure 3a** shows an example of the trial-averaged eye velocity as a function of time for one participant, sorted according to the target velocity profiles (dotted lines) and P(v33) values. Notice that dotted lines indicate horizontal and vertical component velocities (i.e. 7.77 and 23.3 ˚/s for 11 and 33 ˚/s radial speed). A comparison with **Figure 2a** shows a behavior similar to Exp 1 where target motion was horizontal. Final pursuit velocity matches target velocity, at least for the lowest speed (v11) and the highest P(v33) value. The fact that steady-state eye velocity gain remained lower than 1 for the fastest target speed is consistent with previous studies (Carl & Gellman, 1987; Dodge, 1930). More important, as in Exp 1, target motion direction remained constant within a block, an anticipatory pursuit response was always observed. However, its amplitude increased when P(v33) increased. Such dependency is illustrated in **Figure 3b**, where horizontal and vertical components of anticipatory eye velocity

(aSPv) are plotted against P(v33). Both components increased linearly with the probability of the highest speed. A symmetric relationship was observed with P(v11). We ran the LMM statistical models for the anticipatory parameters (aSPv and aSPon), including the effect of P(v33), as for Exp 1. We added effects of eye velocity axes (horizontal or vertical) and their interaction to test whether aSPv was differently modulated along the horizontal and vertical dimensions. aSPv increased significantly for higher probability of P(v33) (**Figure 3b**, P(v33) effect: beta = 2.61, 95% C.I. = (1.42, 3.79), $p < .001$). We also found a significant difference between axes (vertical compared to horizontal axis: beta = -0.84, 95% C.I. = (-1.32, -0.35), $p < .001$), but its interaction with the probability was not significant. This lack of interaction suggests that the directional anisotropy is related to purely oculomotor properties rather than to differences in the expectancy of target radial speed. However, and contrary to Exp 1, we did not find a significant effect of probability or axes on the aSPon. This difference with Exp 1 may be explained by the high variability observed in the estimation of aSPon with the ANEMO method and the higher instrumental noise seen with videoeye trackers, compared to the scleral search coil technique (Drewes et al., 2012). Moreover, our experimental design in naive volunteers resulted in a smaller number of trials, further reducing the statistical power of our results. Yet, the two experiments strongly support the fact that anticipatory eye velocity is scaled by the probability of target speed, independently of the target motion direction.

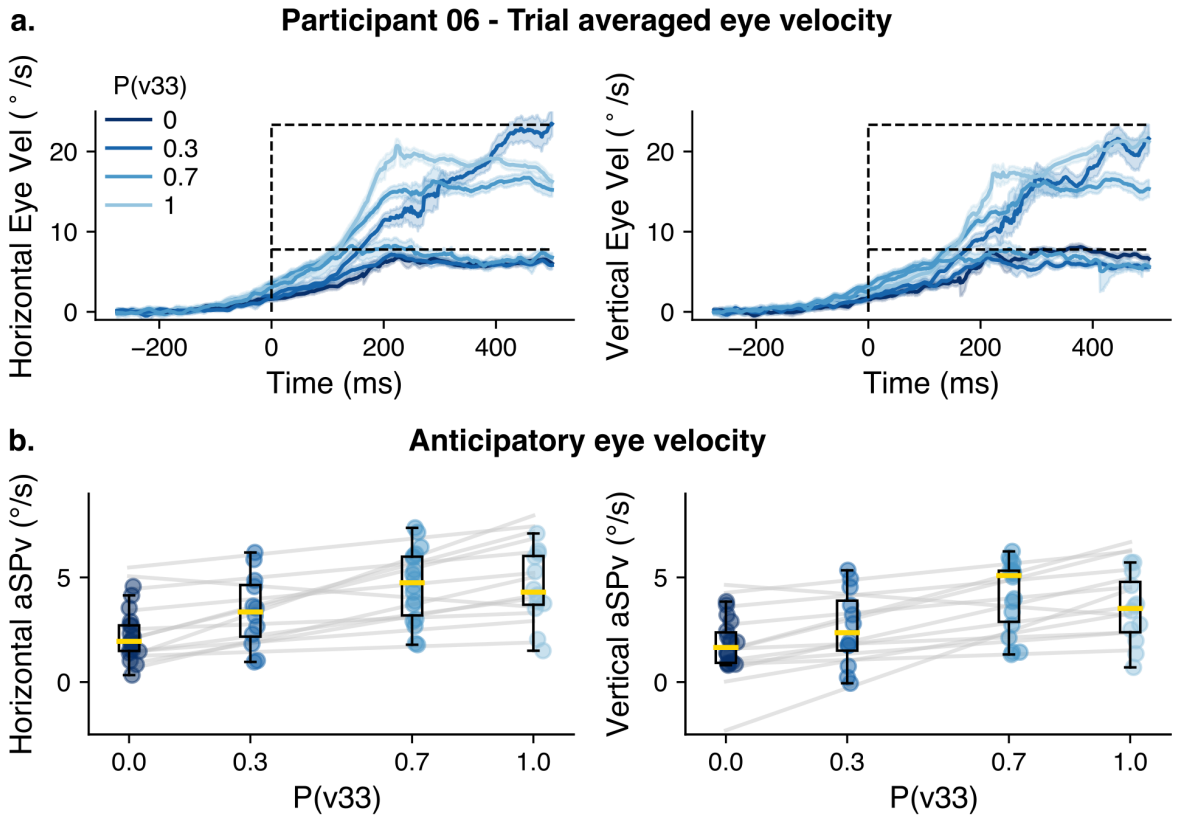

Figure 3. Experiment 2A: Dependence of anticipatory eye velocity upon target speed probability (mixture blocks). **(a).** Average eye velocity for trials grouped by probability of v33 and target velocity for the (v11,v33) mix. The left panel shows the horizontal eye velocity, while the right panel shows the vertical eye velocity for a representative participant. Shades of blue correspond to the different probabilities of v33 (lighter shades for higher probabilities). **(b).** Amplitude of anticipatory pursuit is plotted against P(v33), along the horizontal (left panel) and vertical (right panel) axes. Data represented in the same way as Figure 2.

Effects of the time-varying target kinematic probability on anticipatory eye movements

Following the same reasoning, we tested the effect of the probability of time-varying target kinematics on aSEM. We compared different probabilistic mixtures of trials with accelerating or decelerating target kinematics. Participants

ran blocks of 4 different probability pairs (P(vdec), P(vac)): (0,1), (0.3, 0.7), (0.7, 0.3) and (1,0). We present data according to P(vdec) values as illustrated in **Figure 4**. **Figure 4a** shows horizontal and vertical trial-averaged eye velocities for one participant and each available combination of P(vdec) and target kinematic conditions. Again, each shade of red indicates one probability condition (lighter shades for higher probabilities of P(vdec)) and time zero indicates the target movement onset. We can see clear anticipatory responses, with stronger anticipation occurring for higher probabilities of decelerating motion. After the anticipatory phase, eye velocity traces corresponding to vacc or vdec trials separate and converge to the target's velocity. Notice that the anticipation seen with P(vdec) = 0 (i.e., P(acc) = 1) was particularly small but still significant in participant 6, as in all others. **Figure 4b** illustrates the horizontal and vertical aSPv, as a function of P(vdec), for each participant. There is an increase in the amplitude of anticipatory pursuit as P(vdec) increases, as confirmed by the LMM statistical analysis (P(vdec): beta = 2.25, 95% C.I. = (1.53, 2.97), $p < .001$). Consistently with the previous analysis, we did not find any difference between the constant displacement and the constant duration conditions, but we found that the aSPv was slightly slower in the vertical axis (vertical vs. horizontal effect: beta = -0.61, 95% C.I. = (-1.04, -0.18), $p < .05$). Lastly, we found that aSPon also increased with higher probability of deceleration (P(Vdec): beta = 9.13, 95% C.I. = (0.35, 17.91), $p < .05$).

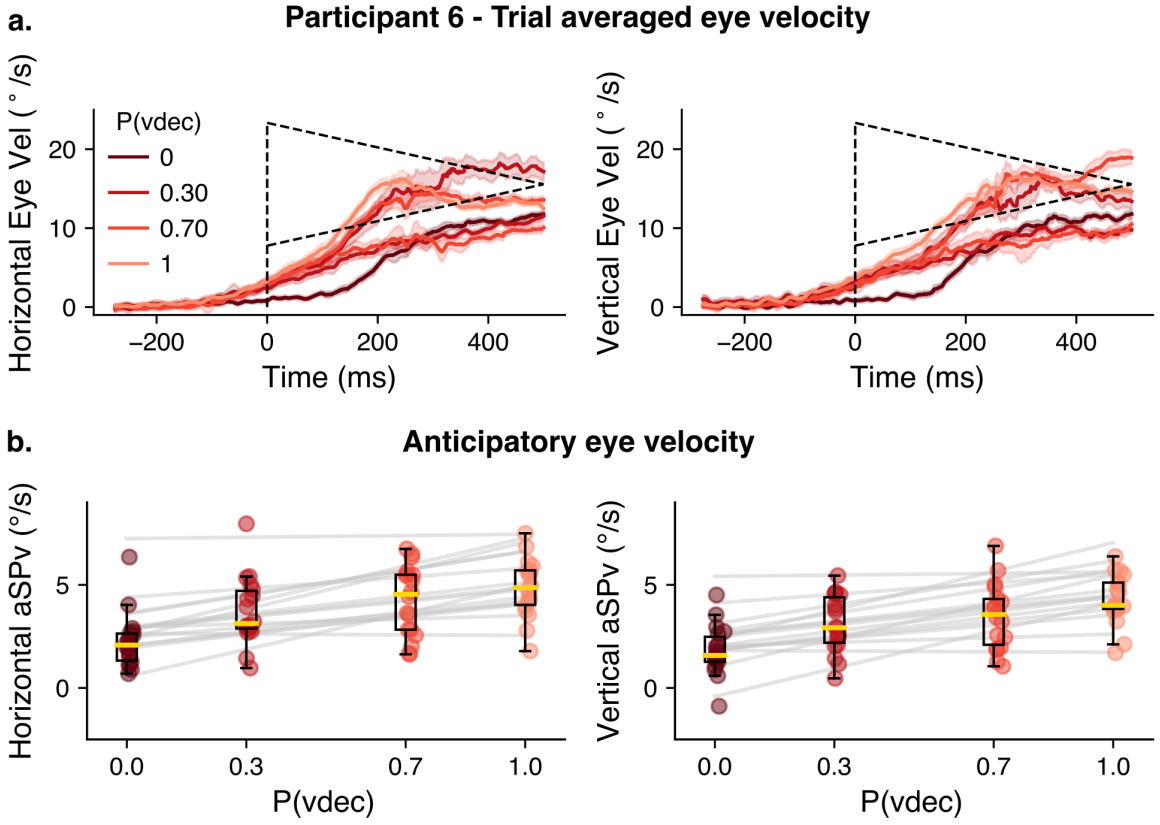

Figure 4. Experiment 2A. Effect of the probability of time-varying target kinematics upon anticipatory eye movements (mixture blocks). **(a).** Average eye velocity across time for a representative participant. Trials are grouped according to the probability of vdec (P(vdec)) and sorted from averaging across trials of different target kinematics for each (P(vdec), P(vacc)) mix. Left and and right panels show horizontal and vertical eye velocity profiles, respectively. Shades of red show the different probabilities of Vdec (lighter shades for higher probabilities). The dashed lines show the target velocity. **(b).** Mean anticipatory eye velocity as a function of the probability of Vdec, group results. Data represented in the same way as Figure 2.

Effects of different target kinematics on anticipatory Smooth Eye Movements

We then addressed the question of how the anticipation for time-varying target kinematics compares to the anticipation for constant target speeds. To do this,

we focused on the fully-predictable blocks and compared three conditions where oblique target motion had a constant speed (v11, v22 and v33, corresponding to radial 11, 22 and 33 °/s, respectively) to a condition in which the target started at v11 and accelerated uniformly (vacc, acceleration = 22 °/s^2) and a condition in which the target decelerated uniformly from the initial velocity v33 (vdec, acceleration = -22 °/s^2). The different target kinematic conditions were presented in a block design, with each condition being repeated over a block of 100 trials, leading to full predictability of target kinematics (P(v11, v22, v33, vacc, vdec) = 1). In addition, we compared two different conditions. In a first version of the experiment (Exp 2A), target displacement was kept constant across blocks, leading to varying target motion durations. In Exp 2B, we conversely kept the target motion duration constant, while allowing for a different target displacement across blocks. The two experiments were analyzed together and, in order to assess whether there were differences between experiments 2A and 2B, LMMs included an interaction effect with the factor “experiment”. **Figure 5a** shows eye velocity profiles recorded in one participant, for Exp 2A, for each of the 5 target kinematic conditions, illustrated by the dotted lines. Since targets were moving along one of the 4 diagonals, we show horizontal and vertical velocities of both eye and target motions, as in **Figure 3a**. Constant speed targets drove strong anticipatory pursuits that were scaled according to target speed. In addition, both accelerating and decelerating conditions also resulted in clear anticipatory pursuit responses, although somewhat smaller for the accelerating target motion condition.

Anticipatory pursuit for the vdec condition was robust and very similar to that observed with the v33 condition.

Figure 5b,c illustrate both the amplitude (aSPv) and onset timing (aSPon) of these anticipatory pursuit responses for the 5 different conditions. Right and left-hand plots show horizontal and vertical components, respectively. Anticipatory eye velocity increases with target constant speed. Moreover, aSPv measured for vdec condition was in-between (and comparable to) the v22 and v33 conditions. Lastly, the amplitude of anticipation was lower for the vacc condition and close to the one elicited by the v11 condition. We ran an LMM model comparing the effects of v11, v22, v33, vacc, and vdec on aSPv and aSPon, with target kinematics as a categorical variable (see Methods and Supplementary material for details). As shown in **Figure 5a**, we found a significant modulation of aSPv by target kinematics. First, aSPv in the constant speed conditions v22 and v33 was significantly higher than in the v11 condition (difference compared to v11, v22: beta = 1.67, 95% C.I. = (0.88, 2.45), $p<.001$; v33: beta = 2.45, 95% C.I. = (1.61, 3.29), $p<.001$)), and aSPv in the condition v33 was higher than in the v22 condition, although not significantly. Indeed, aSPv increased approximately linearly with constant target speed. The aSPv in the accelerating condition (vacc) was significantly lower than for v22, v33 and vdec (difference compared to Vacc, V22: beta = 1.29, 95% C.I. = (0.24, 2.34), $p<.05$); V33: beta = 2.07, 95% C.I. = (1.23, 2.92), $p<.001$; Vdec: beta = 1.78, 95% C.I. = (0.86, 2.70), $p<.001$). It was slightly higher, although not significantly, than aSPv measured in v11. By contrast, aSPv for the decelerating condition (vdec) was significantly higher than v11 (difference compared to Vdec, V11: beta = -2.16,

95% C.I. = (-2.89, -1.43), $p < .001$). Its amplitude was found between v22 and v33 conditions, but not significantly different from both fast target speeds.

When comparing experiments 2A and 2B, we found that anticipatory pursuit velocity (aSPv) with v11, v22 and v33 was faster when target duration was fixed, in comparison to when target displacement was fixed (difference compared to constant displacement, V11: beta = 0.73, 95% C.I. = (0.34, 1.13), $p < .001$; V22: beta = 0.50, 95% C.I. = (0.11, 0.89), $p < .05$; V33: beta = 0.50, 95% C.I. = (0.10, 0.90), $p < .05$). However, we found no significant difference between the two experiments for both time-varying speed conditions (vacc and vdec). We also found no differences between aSPv across the two axes (horizontal vs vertical) for V11, V33 and Vacc, but for V22 and Vdec, aSPv was faster in the horizontal component when compared to the vertical one (difference compared to horizontal, V22: beta = -0.58, 95% C.I. = (-1.05, -0.12), $p < .05$; Vdec: beta = -0.73, 95% C.I. = (-1.19, -0.26), $p < .001$).

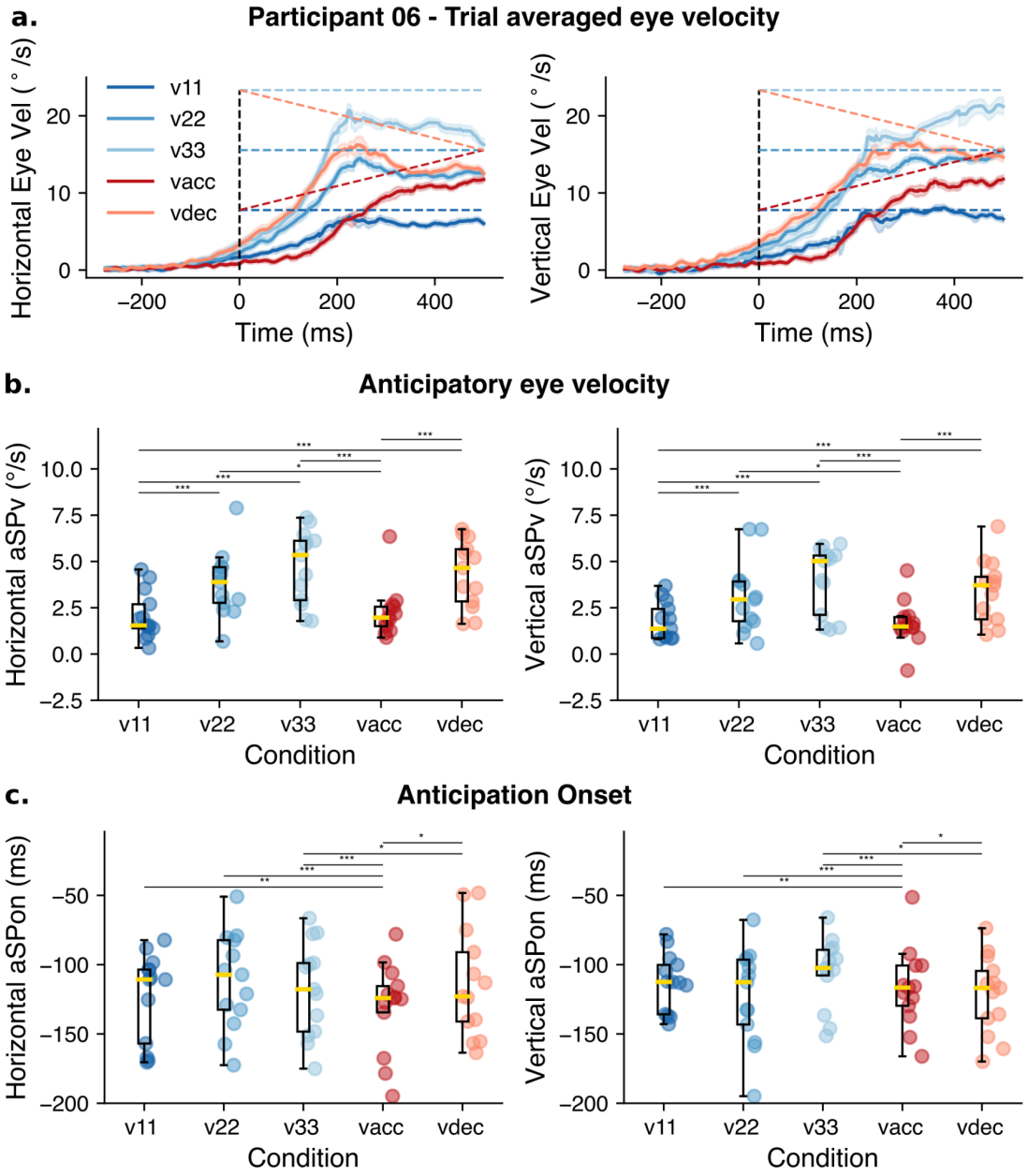

Figure 5. Experiment 2A. Effect of target kinematics on aSEM (fully-predictable blocks). **(a).** Average eye velocity over time with trials grouped by target kinematics-condition for one representative participant. Constant speed target motion conditions are shown in shades of blue, while accelerating target motion conditions are shown in shades of red. The dashed lines show the target speed for the three constant speeds and for the accelerating and decelerating target motions. **(b). and (c).** Group effect of target kinematics on the aSPv (b) and aSPon (c) for both horizontal (left) and vertical (right) components. Horizontal black lines indicate the pairs of conditions which are significantly

different from each other: * $p<.05$; ** $p<.01$; *** $p<.001$. Data are represented in the same format as in Figure 2.

Regarding the anticipatory pursuit onset timing (SPon), there was a strong variability across participants and the effects were overall rather small (range of 5-20 ms across participants and conditions). Moreover, aSPon was not significantly different across the 3 constant speed conditions (v11, v22, and v33). However, anticipatory pursuit started earlier (i.e. aSPon was larger by ~10ms) for an accelerating target (vacc) when compared to all other conditions (difference compared to v11: beta = 7.82, 95% C.I. = (2.03, 13.60), $p<.01$; v22: beta = 9.83, 95% C.I. = (4.29, 15.37), $p<.001$; v33: beta = 11.87, 95% C.I. = (6.41, 17.33), $p<.001$; vdec: beta = 6.21, 95% C.I. = (0.72, 11.70), $p<.05$). It is noteworthy that v11 and vacc yield to different anticipation timing, regardless that speed at target motion onset was the same (11°/s). In the same vein, aSPon was always significantly larger (i.e anticipation onset was earlier) for a decelerating target when compared to the v33 conditions, despite their similar target speed at motion onset (difference compared to Vdec, V33: beta = 5.66, 95% C.I. = (0.39, 10.93), $p<.05$). For comparison, aSPon occurred earlier for vdec when compared to v11 and v22, although these differences were not statistically significant. Regarding potential differences due to horizontal and vertical components or constant duration/displacement conditions, we did not observe any significant effect on aSPon.

In summary, highly predictable target motions along the diagonal directions yield to anticipatory pursuit responses in both horizontal and vertical eye

movements and both with constant or time-varying target speeds. We found a strong and reliable dependency of anticipatory eye velocity upon target kinematics. Timing of anticipatory response onset was also affected, although on a smaller scale and less reliably across conditions and participants. Overall, aSPv was slower for the accelerating condition (vacc) and closer from that observed with the v11 condition than the other constant speeds. Conversely, aSPv was closer to that observed with the v22 and v33 conditions. It must be recalled that (vacc,v11) and (vdec,v33) pairs of conditions share the same target speeds (11 and 33 °/s, respectively) at motion onset. This pattern of results suggest that, with time-varying velocity kinematics, the target velocity estimated during the initial (and not the final) part of the target motion largely determines the amplitude of anticipatory eye velocity. In the next section we perform additional analyses to better characterize the nature of the representation of accelerating/decelerating target motion that might be stored and used in order to control aSEM.

Equivalent target speed estimation for time-varying speed targets

Previous studies investigating predictive smooth pursuit during the transient disappearance of the target have suggested that the internal model of target motion takes into account both the last sample of observed target velocity and its rate of change. However, this was possible only if target displacement properties were estimated during a sufficiently long interval (Bennet et al. 2007) and performance was suboptimal as participants were not able to extrapolate accelerating motion with sufficient accuracy (Bennet & Benguigui 2013). Here, we considered a simpler version of the internal model of target velocity, which only takes into account an

estimate of the mean expected target velocity during a particular time-epoch. We first reasoned that if the aim of aSEM is to minimize the velocity error at the initiation of visually guided pursuit, then aSEM should be proportional to the target velocity during the 0-150 ms period preceding the visually-guided initiation. In this time epoch, the mean target velocity is ~14.5 °/s for vacc and ~30 °/s for vdec. The alternative hypothesis is that aSEM acts to minimize velocity error during steady state pursuit. Then, aSEM should be proportional to the target velocity estimated during a later phase of pursuit. Considering for instance the ~300-400 ms time window after target movement onset, the mean target speed is now of ~19 °/s and ~25 °/s for vacc and vdec, respectively. If the time window used for velocity estimation is even a later one, the estimated target velocity should practically not differ for vacc and vdec (as they converge to an intermediate speed). The results shown in the previous section seem to be more coherent with an internal model taking into account an estimate of the target kinematics in the early epoch of visual motion, as we did not find differences on the aSPv between vacc and v11, nor between vdec and v33, whereas vdec and vacc lead to significantly different anticipatory eye velocity.

To better understand the relationship between aSPv and the internal representation of the target kinematics in the accelerating/decelerating conditions, we ran a new analysis, based on the assumption that an "*equivalent constant speed*" estimation is indeed formed and used to guide anticipatory eye movements. It is known that aSPv scales with constant target speed (e.g. Kao & Morrow, 1994), and we replicated this result. Assuming a linear dependence, it can then be used to

estimate which (equivalent, constant) target speed would have elicited the anticipatory eye velocity observed in the accelerating/decelerating conditions. To eliminate any oculomotor source of variability, we computed back the radial eye velocity for each participant and fitted individual regressions using the constant speed values (v11, v22, v33) as predictors for the mean aSPv. Then, the inverse operation predicts the individual *equivalent target speed* for each participant's mean aSPv measured in the accelerating and decelerating conditions.

Figure 6 illustrates the mean predicted *equivalent target speed* for accelerating and decelerating conditions (in red and orange, respectively) for each participant. The left panel (**Figure 6a**) also shows an estimate of the distribution of the predicted equivalent target speed for the constant target speeds. Such distribution allows to visually estimate the variability of the individual mean regression modeling the aSPv against target speed relationship. Note that the widths of the distributions are large, but there is a clear positive relationship between anticipatory eye velocity and predicted target speed across the constant speed conditions. Regarding the predicted values for the accelerating and decelerating conditions, there is also a very high variability across participants. The predicted *equivalent target speeds* are overall lower for vacc than for vdec, but the individual data points are spread throughout the three 2D distributions of the constant speed conditions. **Figure 6b** illustrates the estimated distribution of the predicted target speed for vacc and vdec. Given the extended superposition of the distributions estimated for different kinematic conditions, it is not possible to conclude in favor of a unique representation format for accelerating/decelerating target motion in the

predictive drive of anticipatory eye movements, at least not at the level of a mean velocity approximation.

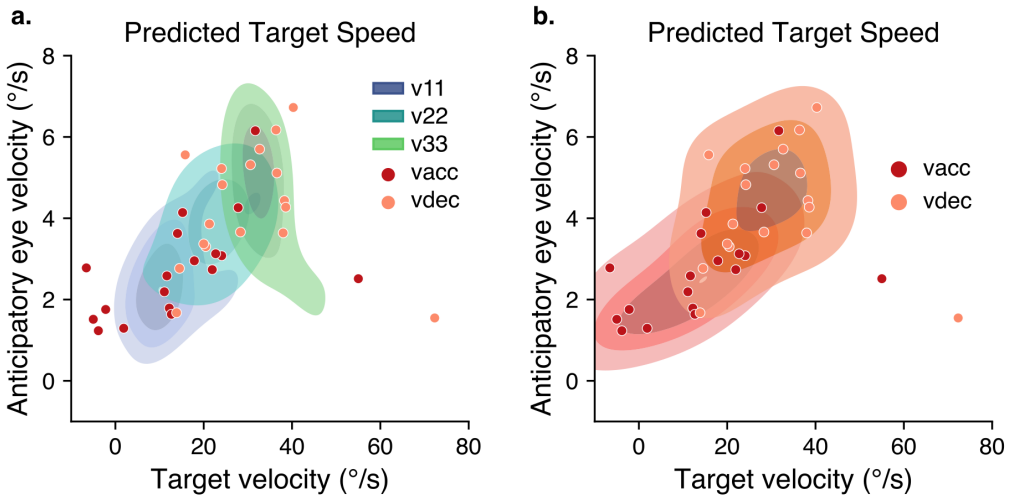

Figure 6. Equivalent target speed estimation. **a.** The density plots show the 2D distributions of anticipatory eye velocity and predicted target speeds for the constant speed conditions, each iso-contour corresponding respectively to 25, 50 and 75 % of the density distribution. The dots correspond to the mean predicted equivalent target speed and mean anticipatory eye velocity for each participant for the accelerating (red) and decelerating (orange) conditions. **b.** The density plots show the 2D distributions of anticipatory eye velocity and predicted equivalent target speeds for the time-varying kinematics conditions.

Retinal velocity error (retinal slip) under different conditions of predictable target kinematics

Next, we asked how anticipatory behavior can be advantageous in terms of tracking performance. Here we focus on a simple descriptive analysis of the retinal velocity error (i.e. target velocity minus the average eye velocity), as the minimization of this quantity has been previously hypothesized as the main goal of

prediction-based anticipatory smooth eye movements (Damasse et al., 2018; Kao & Morrow, 1994). Note also that the minimization of the retinal position error (i.e. the accurate foveation of the moving target) can be reasonably seen as the product of the synergistic coordination of smooth eye movements and catch-up saccades (e.g. Coutinho et al., 2021), which is out of the scope of the present study. **Figure 7** shows, for each participant in the top row and for the group in the bottom row, the mean retinal velocity error for the constant and time-varying kinematic conditions during different phases of the pursuit, from anticipatory (-50 to 0ms), open-loop (150-250ms) and early (300-400ms) and late (400-500ms) closed-loop pursuit phases. Note that we ordered the time-varying velocity conditions based on the average anticipatory pursuit velocity they elicit (see **Figure 5b**): thus vacc lies between v11 and v22 and vdec lies between v22 and v33. Overall, retinal slip increased with increasing constant target speed and reduced over time (blue lines). The temporal dynamics of retinal velocity error differed in the two time-varying speed conditions (orange curves). While it matched that observed with constant speed during anticipatory and open-loop pursuit initiation, it showed no changes with target acceleration conditions for late, closed-loop pursuit phases.

In this later phase, the eye velocity is consistently slower than the target velocity for the accelerating targets, more dramatically than for constant velocity targets leading to comparable eye velocity in the earlier phase. On the other hand, for the decelerating target, the retinal slip is reduced in the late phase of visually-guided pursuit, although this is probably more of a “passive” effect, or, in other terms, it is simply due to the reduction of the target speed across time.

Whereas this descriptive analysis does not allow to clearly elucidate what kind of internal model drives the anticipation of accelerating targets, we can claim that the cost in terms of mean retinal velocity error during the open-loop phase is not very different for time-varying and constant velocity targets when their kinematics is fully predictable.

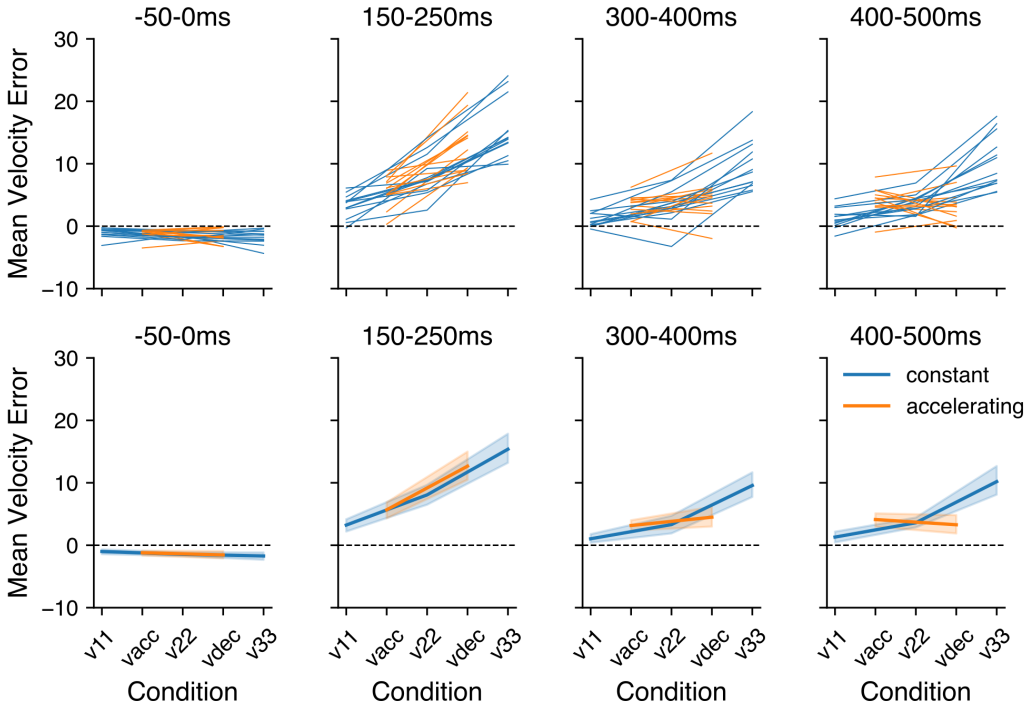

Figure 7. Mean retinal velocity error. The top row shows the mean retinal velocity error for each participant, while the bottom row shows the group average. The mean retinal velocity error is shown for different time windows, roughly corresponding to the anticipatory phase, the open-loop phase and two time windows in the closed-loop phase (from left to right: -50-0 ms, 150-250 ms, 300-400 ms and 400-500ms). The errors for the constant target speeds are shown in blue, while the errors for the accelerating targets are shown in orange.

Effects of the target kinematic probability on the initiation of visually guided pursuit

Our novel dataset and experimental conditions allow us to reconsider how target motion uncertainty affects pursuit initiation driven by visual information about target motion. Thus, we are in a position to compare different target kinematics, with either constant or changing speeds and along either horizontal or diagonal motion directions. Moreover, we can probe how anticipatory pursuit responses would impact pursuit initiation and whether predictive information shapes anticipatory and visually-driven responses in a coordinated way in order to optimally track a moving target. We can do so by estimating the differential effects of a given target speed probability (e.g. P(HS)) on trials where the actual target speed was either consistent (e.g. vHS) or different (e.g. vLS).

Figure 8 illustrates the latency and initial acceleration of visually-driven pursuit, as a function of P(HS), for horizontal target motion (Exp 1). Recall that eye movements were here recorded in 3 highly experienced participants, with the scleral search coil technique. P(HS) (and conversely P(LS)) had little effect on the latency of visually-driven pursuit, but had a strong impact upon initial pursuit acceleration. **Figure 8b** sorts trials according to the actual target speed (HS vs LS, blue vs green curves, respectively), for each P(HS) condition. As the probability for the highest speed (HS) increased, initial pursuit acceleration for the HS trials increased. Conversely, initial pursuit acceleration for the LS trials decreased. We ran LMM models similar to that used above for anticipatory oculomotor parameters

(aSPv, aSPon) but this time with initial pursuit parameters extracted from ANEMO (SPacc, SPlat). However, this time we added the target kinematics (Tk, LS vs HS) as a fixed factor which could interact with the probability. The statistical analysis confirmed that target speed itself, but not speed probability, had an effect on the latency (SPlat), with SPlat being ~5 ms longer for LS trials when compared to HS trials (Tk effect: beta = 4.87, 95% CI = (2.22, 7.52), $p < .001$). More interesting, initial pursuit acceleration (SPacc) was modulated by both current target speed and its probability. SPacc was ~ 45 $^{\circ}/s^2$ lower for LS trials, as compared to HS trials (Tk effect: beta = -45.48, 85% CI = (-55.56, -35.20), $p < .001$). For HS trials, SPacc increased with P(HS) in a dramatic way, (P(HS) effect: beta = 31.94, 95% CI = (23.22, 40.66), $p < .001$), such that the pursuit initial acceleration for a same target speed (HS) was ~30% stronger when that speed was highly predictable. Similarly, for LS trials, SPacc of response to the slow speed target increased with higher P(LS) (P(HS) by Tk interaction effect: beta = -55.32, 95% CI = (-63.74, -46.89), $p < .001$). Overall, uncertainty about target speed changes how visual motion information is processed to drive pursuit initial acceleration.

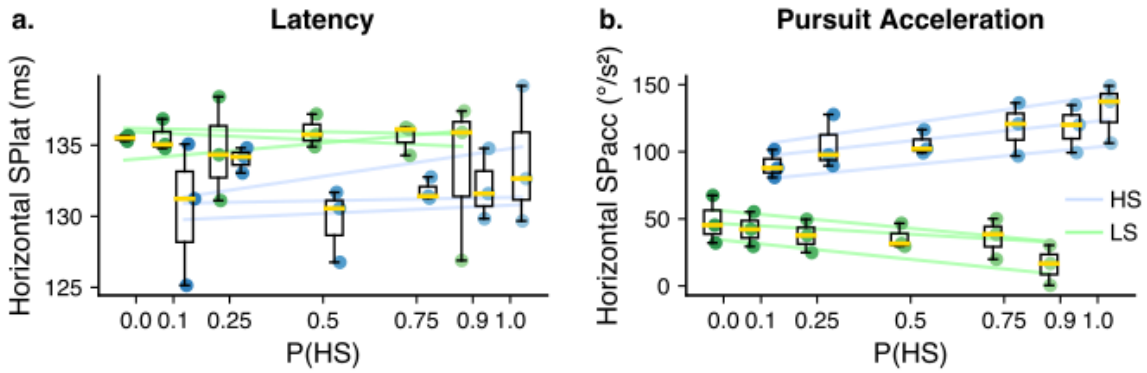

Figure 8. Dependence of the latency and initial acceleration of visually guided pursuit

upon probability and target speed for Experiment 1. **(a).** Group results for SPlat. **(b).** Group results for the SPacc. In all panels, data are separated by target speed (LS trials in green and HS trials in blue). Boxplots represent data in the same way as Figure 2.

Next, we ran a similar analysis for Exp 2A, where v11 and v33 constant speeds were mixed within blocks of diagonal target trajectories. **Figure 9a,b** plots the relationships between horizontal (left) and vertical (right) pursuit latency (a) and acceleration (b) and P(v33). Again, trials were sorted according to the actual target speed (v11: green, v33: blue). First, we can see that SPlat was ~16 ms shorter, and SPacc was ~37 $^{\circ}/s^2$ slower for low-speed (v11) trials as compared to high-speed (v33) trials (difference between v11 and v33, SPlat: beta = -16.15, 95% C.I. = (-20.24, -12.07), $p < .001$; SPacc: beta = -36.91, 95% C.I. = (-48.63, -25.19), $p < .001$). Unexpectedly, target speed probability differently affected pursuit latency and acceleration, dependending upon the speed condition. For v33 speed trials, SPlat decreased with increasing P(v33), SPlat: beta = -19.79, 95% C.I. = (-25.49, -14.09), $p < .001$). However there was no significant effect of P(v33) on pursuit acceleration (SPacc). These non conclusive results for a 33°/s moving target stand in contrast with the significant interaction found with the v11 speed trials. When targets moved at 11°/s, both SPlat and SPacc decreased with increasing P(v11) (i.e., decreasing P(v33), P(v33) by Tk interaction, SPlat: beta = 20.32, 95% C.I. = (15.01, 25.63), $p < .001$; SPacc: beta = 14.30, 95% C.I. = (4.21, 24.38), $p < .01$). These differences with Exp 1 (see **Figure 8**) could possibly be explained by the lower signal-to-noise ratio in the eye position data due to video eye tracking in Exp 2A, as well as by the participation of naive, less trained participants. Moreover, we observed partly different results when considering horizontal and vertical

components of the pursuit initiation (comparison between left and right panels in **Figure 9a**). Indeed, SPacc was significantly higher (~18 °/s^2) in the vertical axis for the v33 speed trials (axis effect: beta = 17.57, 95% C.I. = (8.58, 26.57), p<.001), but ~ 11 °/s^2 lower for the vertical axis with v11 trials (axis by Tk interaction: beta = -11.11, 95% C.I. = (-17.26, -4.96), p<.001). The modulatory effect of P(v33) was smaller along the vertical axis for both SPlat and SPacc (P(v33) and axis interaction, SPlat: beta = 5.41, 95% C.I. = (1.30, 9.51), p<.01; SPacc: beta = -16.80, 95% C.I. = (-26.79, -6.80), p<.001). Altogether, these methodological and data-measurement differences may explain why we failed to reproduce in Exp 2a,b the same pattern of results of Exp 1, and in particular a significant effect of probability upon pursuit initial acceleration.

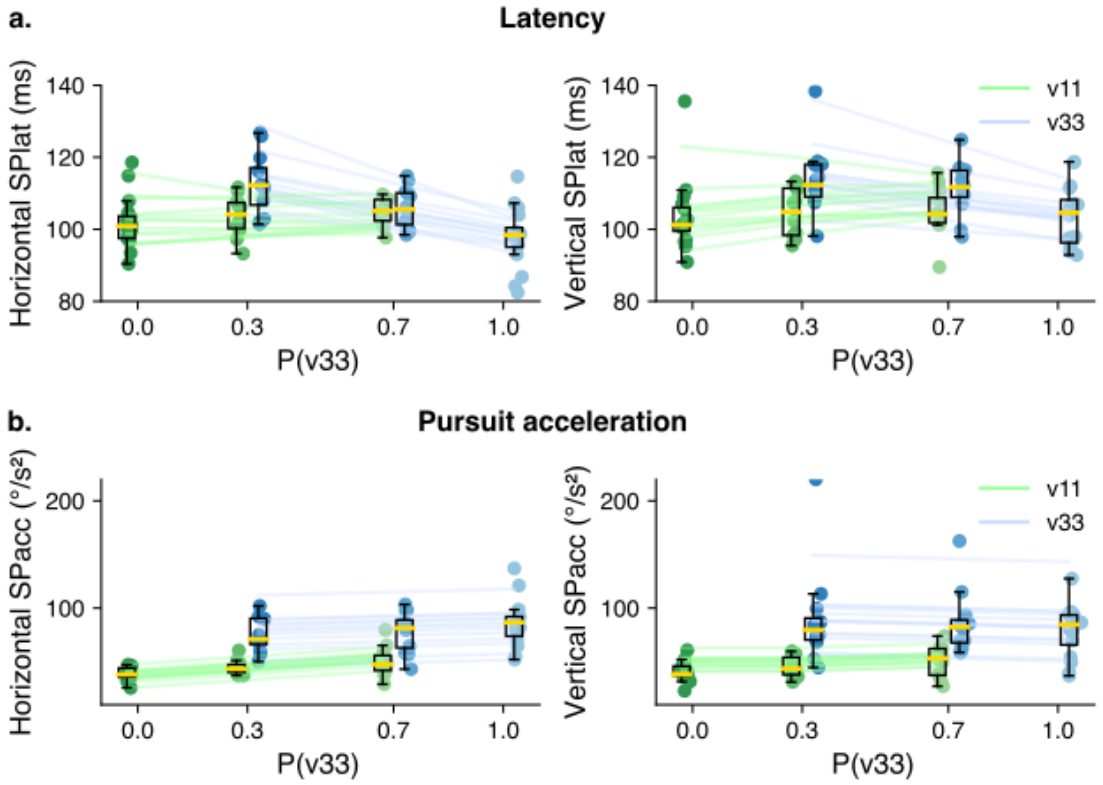

Figure 9. Dependence of the latency and initial acceleration of visually guided pursuit

upon probability and target speed for the constant speed mixes of Exp 2A. **(a).** Group results for SPlat. **(b).** Group results for SPacc. Left panels correspond to the horizontal component and right panels to the vertical component. In all panels, data are separated by target speed (v11 trials in green and v33 trials in blue). Data represented in the same way as Figure 2.

Then, we measured the effects of target acceleration/deceleration probability on pursuit initiation. Similar to the constant speed probabilistic mixtures, latency of both vacc and vdec trials decreased with higher P(vacc) and P(vdec), respectively (P(vdec), vdec trials: beta = -9.06, 95% C.I. = (-13.75, -4.37), $p < .001$; P(vdec) by Tk interaction: beta = 12.07, 95% C.I. = (7.67, 16.47), $p < .001$), and pursuit acceleration was not significantly modulated by the probability levels. We did not find any systematic differences between duration/displacement conditions or between horizontal/vertical axes.

Lastly, we compared constant and changing speed conditions (Exp 2A and 2B). Similar to **Figure 5**, **Figure 10a,b** illustrates pursuit latency and initial acceleration for each condition, estimated from the fully-predictable blocks (P(v11, v33, v22, vacc, vdec) = 1). One can see that initial acceleration (SPacc) was largely affected by both constant and changing speed trajectories. First, we replicate and extend the results of Exp 1: when target velocity (direction and speed) is highly predictable, higher constant speeds (range 11-33°/s) linearly drive higher initial acceleration (**Figure 10b**). LMM analysis indicated, as expected, that SPacc was significantly higher for v22 and v33 than for v11 (compared to v11, v22: beta = 25.75, 95% C.I. = (22.03, 29.48), $p < .001$; v33: beta = 47.05, 95% C.I. = (43.33, 50.77), $p < .001$) and that v33 was significantly higher than v22 (compared to v22,

v33: beta = 21.30, 95% C.I. = (17.67, 24.93), $p < .001$). However, latency was only marginally and partly significantly affected (**Figure 10a**). SPlat was significantly earlier for v33 when compared to v22, but we found no significant difference between v11 and v22, or between v11 and v33 (difference compared to V22, V33: beta = -6.01, 95% C.I. = (-10.09, -1.93), $p < .01$).

By comparing constant and varying speed conditions in **Figure 10**, we can see that pursuit latency varies little between conditions. Indeed, statistical analyses failed to show a consistent pattern. We found that pursuit latency (SPlat) for accelerating targets (vacc) was significantly longer than for both v11 and v33 but not for v22 (v11: beta = -4.02, 95% C.I. = (-7.74, -0.30), $p < .05$; v33: beta = -7.47, 95% C.I. = (-11.38, -3.56), $p < .001$). In the decelerating conditions, SPlat was significantly longer than for v33 (difference compared to Vdec, v33: beta = -3.87, 95% C.I. = (-7.63, -0.11), $p < .05$) but not significantly different from v11 and v22. On the contrary, we observed a consistent pattern of SPacc amplitude across the 5 conditions, very similar to that observed with anticipatory pursuit (aSPv, see **Figure 5**). Pursuit acceleration (SPacc) in the vacc condition was intermediate between v11 and v22 conditions. It was found in between v22 and v33 conditions for the decelerating condition (vdec). We ran the LMM models to check for pairwise statistical differences, indicated by * symbols in **Figure 10b**. When comparing SPacc in the vacc condition to the three constant speeds, we found that it was significantly larger than for v11 (difference compared to vacc, v11: beta = -12.44, 95% C.I. = (-16.18, -8.70), $p < .001$) but smaller than v22 (beta = 13.31, 95% C.I. = (9.66, 16.96), $p < .001$) and v33 (beta = 34.61, 95% C.I. = (30.96,

38.25), $p < .001$). Pursuit acceleration during the accelerating target trials was significantly smaller than during deceleration trials (Vdec: beta = 27.05, 95% C.I. = (23.41, 30.69), $p < .001$). Regarding SPacc during decelerating trials, it was significantly larger than with a v11 (beta = -39.49, 95% C.I. = (-43.20, -35.78), $p < .001$) and v22 constant speeds (beta = -13.74, 95% C.I. = (-17.36, -10.12), $p < .001$) but smaller than with the highest (v33) constant speed (beta = 7.56, 95% C.I. = (3.94, 11.17), $p < .001$).

Finally, we did not find a significant difference in either pursuit acceleration or latency when comparing constant target motion duration/displacement and horizontal/vertical responses.

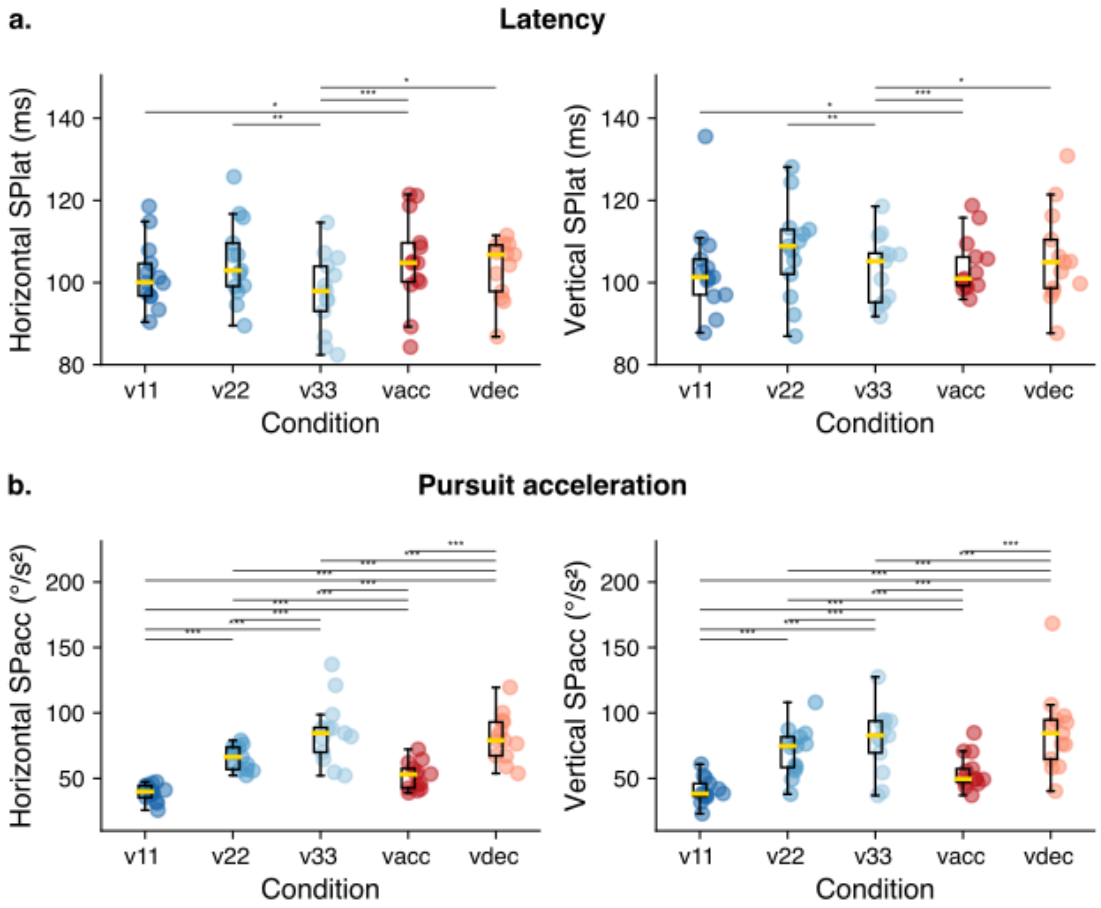

Figure 10. Latency and initial acceleration of the visually guided pursuit dependence upon target kinematics for the Experiment 2. **(a)**. Group results for the SPlat. **(b)**. Group results for the SPacc. Left panels correspond to the horizontal component and right panels to the vertical component. Data represented in the same way as Figure 5.

Discussion

We had two main objectives with the present study. First, we wanted to analyze the effects of a parametric change of the target speed probability upon human anticipatory smooth eye movements. We have done this by re-analysing previously collected data (see Souto et al., 2008) and by replicating and generalizing those results in a larger group of participants and slightly different conditions. In particular, we used target motion trajectories along both horizontal and oblique

directions but kept target motion direction constant within blocks. We also compared different target kinematics, namely constant or time-varying (accelerating or decelerating) target speeds. We found that anticipatory responses were strongly modulated by both constant and varying target speeds. We report a linear scaling of anticipatory pursuit with target speed, similar to what we previously reported for direction. Second, we probed how these different probabilistic cues may shape both anticipatory and visually-driven pursuit eye movements. We report that the initiation of visually-guided pursuit is dependent on the interaction of target speed and target speed probability, suggesting that the probabilistic representations of motion cues can also affect the visuomotor transformation that drives pursuit eye movements.

A linear dependence between anticipatory pursuit and probability of target kinetic cues

In two separate experiments, we showed that the velocity of anticipatory pursuit is modulated by the constant-speed probability of visual moving targets, regardless of its fully predictable direction. These results are consistent with previous reports (as reviewed in Kowler et al., 2019) that showed that anticipatory smooth velocity is modulated by the predictability of target speed. Our results are however novel on two aspects. First, we demonstrate a parametric, linear relationship between amplitude of the anticipatory phase and the full range of target speed probability. Such a linear relationship is present over a broad range of target speeds (from 5 to above 30°/s) and is similar for targets moving along either

the horizontal (**Figure 2**) or the oblique axes (**Figure 3**). It has been shown previously that anticipatory responses to expected target motion are stronger for targets at higher speed (Heinen et al., 2005; Kao & Morrow, 1994; Maus et al., 2015). Here we report for the first time that anticipatory pursuit is affected by both target speed and its probability in a parametric way. Higher order kinetic cues such as acceleration or deceleration rates of varying-speed trajectories can also modulate eye velocity during anticipatory pursuit, again regardless of the (predictable) target motion direction. Such an effect is also modulated by the probability of these different higher-order kinetic cues (**Figure 4**), although the slope of the relationship was slightly shallower. Overall, these novel results extend the previous findings of a linear dependence of the anticipatory eye velocity upon the target direction probability (Damasse et al., 2018; Santos & Kowler, 2017) and further demonstrate that the statistical regularities of different motion properties are efficiently stored and processed for anticipatory visuomotor control. Our results argue for a probabilistic coding of target velocity (direction and speed) but future work is needed to elucidate whether these aspects of target trajectories are encoded together or separately. Nevertheless, anticipatory eye movements appear as an effective approach to elucidate how direction and kinematic parameters are encoded to control eye movements.

Second, using the most sensitive oculomotor recording technique in highly experienced participants (the scleral search coil technique), we found that the timing of anticipatory responses is also linearly modulated by target speed probability. This effect was consistent, with anticipatory pursuit starting earlier by

~20ms (relative to target motion onset) when target speed was fully predictable. The timing of anticipatory responses has been previously related to the probabilistic encoding of target timing itself and to the presentation of timing-cues during a fixation-motion gap paradigm (Badler & Heinen, 2006) or a repeated target motion ramp paradigm (Barnes & Donelan, 1999). Although we did not compare different cueing conditions, here we evidence that both strength and timing of anticipatory responses are scaled (the stronger and the earlier) by target speed probability.

However, in Experiment 2, we could not replicate the significant effect of speed probability upon the onset timing of the oculomotor anticipation. Since we found that the strength of anticipatory responses was not different between different motion directions and that the range of target speeds was overlapping between the two experiments, we can probably reject the possibility that this discrepancy is due to differences in target motion properties. It may however be explained by differences between experimental methods. First, the estimate of the anticipatory onset is inherently a noisy measure, even more so when based on the video eye tracker (like in Exp 2), compared to the scleral search coil technique (Exp 1), which has a much higher signal-to-noise ratio. Second, there was a reduced statistical power in the design of the second experiment compared to the first one: we had actually a smaller number of trials per condition. The larger number of participants, mostly naive, was not sufficient to compensate for these experimental factors and future work using higher signal-to-noise ratio measurements and statistical power shall be conducted in the future to confirm our results. More robust evidence in this sense would also allow us to understand whether or not timing and kinetic

parameters of target motion are jointly or separately encoded in a probabilistic framework (Badler & Heinen, 2006; Barnes & Donelan, 1999).

An internal representation of time-varying target kinematics

In this study, we show that accelerating and decelerating targets yield different eye velocities during anticipatory responses. Target motion conditions were designed such that constant speeds can be compared with varying speed conditions: speeds at target motion onset were similar for fast (33 °/s) and decelerating speed conditions as well as for slow (11 °/s) and accelerating speed conditions. An intermediate constant speed equal to 22 °/s was also presented in fully predictable blocks. Despite that the target started moving at the same high/low speed, decelerating and accelerating predictable target motion modulated anticipatory eye velocity in a specific way. The quantitative comparisons indicated that anticipatory eye velocity was not simply scaled based on the initial (i.e. 11 ou 33°/s) nor the mean (22°/s) target speed (**Figure 5**). Our additional exploratory analysis based on the estimate of the *equivalent target speed* corresponding to individual anticipatory eye velocity measured with accelerating/decelerating targets (**Figure 6**) further confirmed this observation. The estimated equivalent target speed was actually very variable across participants, suggesting that the representation of time-varying speed motion for the oculomotor drive is not related in a simple and unique way to the initial or the time-averaged target velocity. Moreover, the total displacement or duration of target motion had no systematic influence on anticipation. Lastly, anticipatory eye velocity scaled with the

probability of a given target acceleration or deceleration (**Figure 4**). Altogether, and despite the need to further understand the nature of the internal representation of accelerating motion, these results suggest that target speed profile can be used to control anticipatory pursuit, in a probability-dependent manner. Thus, humans can learn the regularities of target trajectories from different cues, such as direction, speed and change in speed.

Whether or not acceleration of moving target is represented and used by the primate tracking system is still unclear (Lisberger & Movshon, 1999), despite the fact that target acceleration is a key component of most current models of smooth pursuit eye movements (Goldreich et al., 1992). In humans, several previous studies have attempted to demonstrate a role for acceleration and whether such high order motion cues can be learned through the history of target motion. Bennett & Barnes (2006) probed predictive smooth pursuit of accelerating targets, using the target transient occlusion paradigm. They reported that, in highly predictable cases, anticipatory eye velocity occurring before the end of target blanking was scaled to the target acceleration. However, increasing uncertainty of target acceleration, by mixing trials, canceled such dependency. Later on, Bennett et al. (2007) showed that when smoothly pursuing an accelerating target which undergoes an occlusion after a short exposition (200 ms), human participants are not able to adaptively use the acceleration information. Instead, they seem to store the estimate of a constant velocity and use saccades to compensate for the displacement error between the eye position and the location where the target reappears. They found, however, that after a longer exposure (500-800 ms, comparable to our visual motion duration),

smooth pursuit and saccades discriminate between the different acceleration profiles. Still, prediction of the target position at the end of the occlusion was not optimal. Other studies came to the same conclusion: acceleration information can be used to somehow control tracking eye (and hand) movements but not to build predictive motor responses to moving targets, or related perceptual judgements (Kreyenmeier et al. 2022).

How motion acceleration is estimated and represented is still disputed. Early psychophysical studies have shown that the mean speed estimated over the stimulus motion duration influences the perceptual discrimination of acceleration (Brouwer et al., 2002; Gottsdanker et al., 1961; Schmerler, 1976). Watamaniuk & Heinen (2003) showed that this is also the case when judging and tracking an accelerated moving target. In addition, the duration of the temporal window during which the target kinematic information is acquired seems to influence the accuracy of acceleration estimation (Bennett et al., 2007). Here, we did not find any difference between constant target motion duration and constant target motion displacement (Exp 2A and 2B) for accelerating targets. In contrast, we found that anticipatory eye velocity is stronger for constant target speeds when the target motion duration is held constant. These results suggest that the exposure time is more important to learn steady target velocity than its acceleration in order to drive and control anticipatory responses. This finding will need to be elucidated by future investigation. For instance, a systematic investigation of the critical temporal integration window for anticipatory eye movements with time-varying target speed is still lacking. We also need a more complete understanding of how speed and

acceleration cues can be integrated through learning sensorimotor contingencies in specific tasks. A very peculiar example is the vertical tracking of a target that changes speed by following the gravity acceleration (Zago et al., 2010). What is being learned, and how to drive anticipatory pursuit responses question the interactions between predictive and sensory information for an optimal tracking behavior. In addition, in alternative or in parallel to the internal representation of the retinal target speed and acceleration, the retinal velocity error could also be estimated and eventually minimized over trials to improve tracking performance. We can speculate that participants could simply learn by trial and error and adapt their anticipation behavior in order to rapidly minimize the difference between the gaze and target velocity. This hypothesis is qualitatively supported by our analysis of the average velocity error during the open-loop and later phases of visually-guided tracking (**Figure 7**): the velocity error seems to be similarly minimized during the early open-loop phase for comparable constant and time-varying speed. This observation suggests that regardless of the detailed representation of accelerating motion, adaptive anticipatory behavior allows just the efficient reduction of that error. Again, this sort of cost-minimization process remains to be thoroughly tested by future model-based experiments.

Integration of predictive and visually-guided information about target kinematics

In order to investigate how predictive information interacts with sensory driven pursuit components, we investigated how probability-based expectation of

different motion cues affect early visuomotor control. Smooth pursuit initiation, in particular its latency and acceleration, primarily depend on the kinematic properties of the visual moving target (Carl & Gellman, 1987). However, when reliable extra-retinal, predictive information is available, it can also affect oculomotor visual tracking, in agreement with the predictions of the Bayesian model of integration of sensory and prior information (Bogadhi et al., 2013; Darlington et al., 2018; Deravet et al., 2018; Orban De Xivry et al., 2013). These previous empirical and computational studies have indeed suggested that eye velocity is controlled by an internal estimate of target velocity that reflects a reliability-weighted integration between the sensory evidence (the target visual motion) and the expected velocity (the *prior*, shaped by experience and by the context). Along the same lines, the ocular tracking control system has been seen as an instantiation of a Kalman sensorimotor filtering (Orban de Xivry et al, 2013, Bogadhi et al., 2013). The present experiments were not designed to explicitly test the reliability-based combination of prior and sensory evidence. Nevertheless, using probabilistic mixtures of targets moving with constant (or accelerating) speed, our present results provide further support of this Bayesian integration hypothesis. Smooth pursuit latency was in general (but not in all conditions) shorter and acceleration always larger for higher speed targets compared to slower ones, as well established since decades (Carl & Gellman, 1987). Yet, for high speed target trials, the latency decreased when the probability of high-speed trials increased, while the latency of slow speed trials increased concurrently (in Exp2, not significantly in Exp1; similar significant effects were also found also for the mixture of accelerating/decelerating

targets). Likewise, the open-loop acceleration of high speed trials increased further with high speed probability, while the acceleration of slow-speed trials decreased. Although the dependence on probability was not significant across all conditions, the overall pattern of results suggest that the initial, open-loop visuomotor transformation driving pursuit initiation is also affected by target predictability. Thus, visually guided pursuit follows the expected pattern predicted by a Bayesian integration framework in which the visual input velocity is combined with prior knowledge, with a stronger modulation of the prior when the probability of the observed motion condition is larger. It is already known that optimal integration can be based on different visual cues about target motion trajectory, such as position, velocity and acceleration, in order to reduce neural delays (Khoei et al., 2017) or optimize sensorimotor transformations (Orban De Xivry et al., 2013). On the other hand, several studies have shown the sub-optimal use of higher-order motion cues for trajectory prediction in the context of hand or eye movements (Bennett, Orban De Xivry, et al., 2010; Kreyenmeier et al., 2022; Watamaniuk & Heinen, 2003; Werkhoven et al., 1992). The present results argue in favor of a significant, although limited role of target motion acceleration in both anticipatory smooth eye movements ahead of target motion onset, as well as in the early phase of the visually-guided ocular tracking. Future computational work shall elucidate how dynamical multi-dimensional representations (i.e. direction, position, speed, acceleration) of target trajectories weigh sensory and predictive motion information for optimal sensorimotor tracking.

Neuronal bases of predictive tracking and processing of different kinematic properties

Electrophysiological studies in the non-human primates have provided evidence that a small subpart of the Frontal Eye Fields (FEFsem, slightly ventral compared to the saccadic FEF) is implicated in the control of predictive smooth pursuit (e.g. Fukushima et al., 2002; MacAvoy et al., 1991, see Kowler, 2019 for a review). Darlington et al. (2018) showed that FEFsem firing rate is modulated, before visual motion onset, by the expectations about the target speed. In addition, the speed-context modulation of neuronal activity continues throughout the visually-guided phase of smooth pursuit, and it is stronger when the visual stimuli are less reliable (i.e. at lower contrast), in agreement with a Bayesian-like integration of prior beliefs and sensory evidence. Such integration was also apparent in the oculomotor recordings, with the monkeys' smooth pursuit eye velocity more strongly modulated by the speed context for low-contrast targets. Unfortunately, the authors could not compare the FEF preparatory activity with anticipatory eye velocity, nor did they analyze the smooth pursuit latency dependence on motion expectancy, thereby limiting the possibility to draw a correspondence with our results. A second prefrontal oculomotor field, The Supplementary Eye Fields (SEF) is also involved in the control of predictive smooth pursuit (Heinen & Liu, 1997). For instance, de Hemptinne et al. (2008) showed that the activity of a population of SEF neurons encoded the target direction expectations, as neurons became more active after the presentation of a cue indicating deterministically a target motion in the neuron's preferred direction. The evidence for the neural substrates of predictive

pursuit is much sparser in humans: Gagnon et al., 2006, have applied transcranial magnetic stimulation (TMS) pulses to the human FEFsem and SEF regions during visual tracking of sinusoidal target motion. They have reported an enhancement of predictive pursuit when TMS was applied to FEFsem at different epochs, but only in some specific conditions when TMS was applied to SEF. Several questions remain yet unanswered. First, the respective role of FEFsem and SEF in predictive eye movement is still debated. Second, how the different variables of target motion trajectories are encoded and learned is yet to be investigated. Thanks to its fast, block-designed protocole mixing different target motion cues, the present study may inspire future neurophysiological studies in non-human and human primates, focusing on the joint analysis of anticipatory responses and preparatory neural activities in these two prefrontal areas.

Our results call for a reevaluation of the role of higher-order motion cues (acceleration/deceleration) in the control and learning of pursuit responses. There is very little evidence that the primate nervous system encodes visual acceleration explicitly, in the visual or in the oculomotor systems. Lisberger & Movshon (1999) measured MT neurons' responses to image acceleration, but did not find evidence that those neurons' activity varied with acceleration. They found, however, that the coupled responses of a population of MT neurons was correlated to image acceleration. On the other hand, they did not find evidence that MT population signals could encode image deceleration. Similarly, Price et al. (2005) found speed tuning in MT single neurons, but not an acceleration or deceleration tuning. However, Schlack et al. (2007) showed that a linear classifier can extract

acceleration signals from the MT population response, given that the MT neurons' tuning to speed depended on the acceleration and deceleration contexts of the task. Note, however, that these earlier studies focused mainly on primate area MT while other parietal (MST) and frontal (FEF) cortical areas might contribute to represent complex target motion trajectories and higher-order kinematics. Future work shall elucidate how position, velocity and acceleration cues are jointly or independently encoded across the visuo-oculomotor distributed network, in order to represent and learn target trajectories for the efficient control of action.

Conclusion

In this study, we showed that when the target speed is predictable, human participants show a linear dependance of anticipatory eye velocity with the speed probability that is comparable to the one found for target direction predictability. Moreover, participants also show anticipatory responses adjusted to time-varying target kinematics, also when the latter are again modulated in terms of across-trials probability. We also reported evidence that the open-loop phase of the visually-guided pursuit is modulated by a combination of the target kinematic predictability and the target motion visual properties, akin to the Bayesian integration framework. Overall, this study contributes to the broad existing literature about the sensory and cognitive control of eye movements by better characterizing the role of predictive information about the target kinematics.

Data availability statement

The data and analysis scripts are available ([link upon acceptance]).

References

Badler, J. B., & Heinen, S. J. (2006). Anticipatory movement timing using prediction and external cues. *Journal of Neuroscience*, *26*(17), 4519–4525.

Barnes, G. R., & Asselman, P. T. (1991). The mechanism of prediction in human smooth pursuit eye movements. *The Journal of Physiology*, *439*(1), 439–461. https://doi.org/10.1113/jphysiol.1991.sp018675

Barnes, G. R., & Donelan, S. F. (1999). The remembered pursuit task: Evidence for segregation of timing and velocity storage in predictive oculomotor control. *Experimental Brain Research*, *129*(1), 57–67. https://doi.org/10.1007/s002210050936

Barr, D. J., Levy, R., Scheepers, C., & Tily, H. J. (2013). Random effects structure for confirmatory hypothesis testing: Keep it maximal. *Journal of Memory and Language*, *68*(3), 255–278. https://doi.org/10.1016/j.jml.2012.11.001

Benguigui, N., & Bennett, S. J. (2010). Ocular pursuit and the estimation of time-to-contact with accelerating objects in prediction motion are controlled independently based on first-order estimates. *Experimental Brain Research*, *202*(2), 327–339. https://doi.org/10.1007/s00221-009-2139-0

Bennett, S. J., & Barnes, G. R. (2006). Smooth ocular pursuit during the transient disappearance of an accelerating visual target: The role of reflexive and voluntary control. *Experimental Brain Research*, *175*(1), 1–10. https://doi.org/10.1007/s00221-006-0533-4

Bennett, S. J., & Benguigui, N. (2013). Is Acceleration Used for Ocular Pursuit and Spatial Estimation during Prediction Motion? *PLoS ONE*, *8*(5), e63382. https://doi.org/10.1371/journal.pone.0063382

Bennett, S. J., De Xivry, J. J. O., Lefèvre, P., & Barnes, G. R. (2010). Oculomotor prediction of accelerative target motion during occlusion: Long-term and short-term eVects. *Experimental Brain Research*, *204*(4), 493–504. https://doi.org/10.1007/s00221-010-2313-4

Bennett, S. J., de Xivry, J.-J. O., Barnes, G. R., & Lefèvre, P. (2007). Target Acceleration Can Be Extracted and Represented Within the Predictive Drive to Ocular Pursuit. *Journal of Neurophysiology*, *98*(3), 1405–1414. https://doi.org/10.1152/jn.00132.2007

Bennett, S. J., Orban De Xivry, J.-J., Lefèvre, P., & Barnes, G. R. (2010). Oculomotor prediction of accelerative target motion during occlusion: Long-term and short-term effects. *Experimental Brain Research*, *204*(4), 493–504. https://doi.org/10.1007/s00221-010-2313-4

Bogadhi, A. R., Montagnini, A., & Masson, G. S. (2013). Dynamic interaction between retinal and extraretinal signals in motion integration for smooth pursuit. *Journal*

of Vision, *13*(13), 5–5. https://doi.org/10.1167/13.13.5

Brainard, D. H. (1997). The Psychophysics Toolbox. *Spatial Vision*, *10*(4), 433–436.

Brouwer, A.-M., Brenner, E., & Smeets, J. B. J. (2002). Perception of acceleration with short presentation times: Can acceleration be used in interception? *Perception & Psychophysics*, *64*(7), 1160–1168. https://doi.org/10.3758/BF03194764

Carl, J. R., & Gellman, R. S. (1987). Human smooth pursuit: Stimulus-dependent responses. *Journal of Neurophysiology*, *57*(5), 1446–1463. https://doi.org/10.1152/jn.1987.57.5.1446

Coutinho, J. D., Lefèvre, P., & Blohm, G. (2021). Confidence in predicted position error explains saccadic decisions during pursuit. *Journal of Neurophysiology*, *125*(3), 748–767. https://doi.org/10.1152/jn.00492.2019

Damasse, J., Perrinet, L. U., & Montagnini, A. (2018). *Reinforcement effects in anticipatory smooth eye movements*. *18*(2018), 1–18.

Darlington, T. R., Beck, J. M., & Lisberger, S. G. (2018). Neural implementation of Bayesian inference in a sensorimotor behavior. *Nature Neuroscience*, *21*(10), 1442–1451. https://doi.org/10.1038/s41593-018-0233-y

de Hemptinne, C., Lefevre, P., & Missal, M. (2008). Neuronal bases of directional expectation and anticipatory pursuit. *Journal of Neuroscience*, *28*(17), 4298–4310.

Deravet, N., Blohm, G., De Xivry, J.-J. O., & Lefèvre, P. (2018). Weighted integration of short-term memory and sensory signals in the oculomotor system. *Journal of Vision*, *18*(5), 16. https://doi.org/10.1167/18.5.16

Dodge, R. (1930). OPTIC NYSTAGMUS: III. CHARACTERISTICS OF THE SLOW PHASE. *Archives of Neurology & Psychiatry*, *24*(1), 21. https://doi.org/10.1001/archneurpsyc.1930.02220130024002

Drewes, J., Masson, G. S., & Montagnini, A. (2012). Shifts in reported gaze position due to changes in pupil size: Ground truth and compensation. *Proceedings of the Symposium on Eye Tracking Research and Applications*, 209–212. https://doi.org/10.1145/2168556.2168596

Fukushima, K., Fukushima, J., Warabi, T., & Barnes, G. R. (2013). Cognitive processes involved in smooth pursuit eye movements: Behavioral evidence, neural substrate and clinical correlation. *Frontiers in Systems Neuroscience*, *7*. https://doi.org/10.3389/fnsys.2013.00004

Fukushima, K., Yamanobe, T., Shinmei, Y., Fukushima, J., Kurkin, S., & Peterson, B. W. (2002). Coding of smooth eye movements in three-dimensional space by frontal cortex. *Nature*, *419*(6903), 157–162.

Gauthier, G. M., Vercher, J. L., Mussa Ivaldi, F., & Marchetti, E. (1988). Oculo-manual tracking of visual targets: Control learning, coordination control and coordination model. *Experimental Brain Research*, *73*(1), 127–137. https://doi.org/10.1007/BF00279667

Goldreich, D., Krauzlis, R. J., & Lisberger, S. G. (1992). Effect of changing feedback delay on spontaneous oscillations in smooth pursuit eye movements of monkeys. *Journal of Neurophysiology*, *67*(3), 625–638. https://doi.org/10.1152/jn.1992.67.3.625

Gottsdanker, R., Frick, J. W., & Lockard, R. B. (1961). IDENTIFYING THE ACCELERATION OF VISUAL TARGETS. *British Journal of Psychology*, *52*(1), 31–42. https://doi.org/10.1111/j.2044-8295.1961.tb00765.x

Grasse, K. L., & Lisberger, S. G. (1992). Analysis of a naturally occurring asymmetry in vertical smooth pursuit eye movements in a monkey. *Journal of Neurophysiology*, *67*(1), 164–179. https://doi.org/10.1152/jn.1992.67.1.164

Heinen, S. J., Badler, J. B., & Ting, W. (2005). Timing and velocity randomization similarly affect anticipatory pursuit. *Journal of Vision*, *5*(6), 1–1. https://doi.org/10.1167/5.6.1

Heinen, S. J., & Liu, M. (1997). Single-neuron activity in the dorsomedial frontal cortex during smooth-pursuit eye movements to predictable target motion. *Visual Neuroscience*, *14*(5), 853–865. https://doi.org/10.1017/S0952523800011597

Hlavac, M. (2022). *stargazer: Beautiful LATEX, HTML and ASCII tables from R statistical output* [R].

Jarrett, C. B., & Barnes, G. (2002). Volitional scaling of anticipatory ocular pursuit velocity using precues. *Cognitive Brain Research*, *14*(3), 383–388. https://doi.org/10.1016/S0926-6410(02)00140-4

Kao, G. W., & Morrow, M. J. (1994). The relationship of anticipatory smooth eye movement to smooth pursuit initiation. *Vision Research*, *34*(22), 3027–3036. https://doi.org/10.1016/0042-6989(94)90276-3

Ke, S. R., Lam, J., Pai, D. K., & Spering, M. (2013). Directional Asymmetries in Human Smooth Pursuit Eye Movements. *Investigative Opthalmology & Visual Science*, *54*(6), 4409. https://doi.org/10.1167/iovs.12-11369

Khoei, M. A., Masson, G. S., & Perrinet, L. U. (2017). The Flash-Lag Effect as a Motion-Based Predictive Shift. *PLOS Computational Biology*, *13*(1), e1005068. https://doi.org/10.1371/journal.pcbi.1005068

Körding, K. P., & Wolpert, D. M. (2004). Bayesian integration in sensorimotor learning. *Nature*, *427*(6971), 244–247. https://doi.org/10.1038/nature02169

Kowler, E., Rubinstein, J. F., Santos, E. M., & Wang, J. (2019). Predictive Smooth Pursuit Eye Movements. *Annual Review of Vision Science*, *5*(1), 223–246. https://doi.org/10.1146/annurev-vision-091718-014901

Kowler, E., & Steinman, R. M. (1979a). The effect of expectations on slow oculomotor control—I. Periodic target steps. *Vision Research*, *19*(6), 619–632. https://doi.org/10.1016/0042-6989(79)90238-4

Kowler, E., & Steinman, R. M. (1979b). The effect of expectations on slow oculomotor control—II. Single target displacements. *Vision Research*, *19*(6), 633–646. https://doi.org/10.1016/0042-6989(79)90239-6

Kreyenmeier, P., Kämmer, L., Fooken, J., & Spering, M. (2022). Humans Can Track But Fail to Predict Accelerating Objects. *Eneuro*, *9*(5), ENEURO.0185-22.2022. https://doi.org/10.1523/ENEURO.0185-22.2022

Landelle, C., Montagnini, A., Madelain, L., & Danion, F. (2016). Eye tracking a self-moved target with complex hand-target dynamics. *Journal of Neurophysiology*, *116*(4), 1859–1870. https://doi.org/10.1152/jn.00007.2016

Lisberger, S. G., & Movshon, J. A. (1999). Visual motion analysis for pursuit eye movements in area MT of macaque monkeys. *The Journal of Neuroscience: The Official Journal of the Society for Neuroscience*, *19*(6), 2224–2246. https://doi.org/10.1523/JNEUROSCI.19-06-02224.1999

Lisberger, S., & Westbrook, L. (1985). Properties of visual inputs that initiate horizontal smooth pursuit eye movements in monkeys. *The Journal of Neuroscience*, *5*(6), 1662–1673. https://doi.org/10.1523/JNEUROSCI.05-06-01662.1985

MacAvoy, M. G., Gottlieb, J. P., & Bruce, C. J. (1991). Smooth-Pursuit Eye Movement Representation in the Primate Frontal Eye Field. *Cerebral Cortex*, *1*(1), 95–102. https://doi.org/10.1093/cercor/1.1.95

Maus, G. W., Potapchuk, E., Watamaniuk, S. N. J., & Heinen, S. J. (2015). Different time scales of motion integration for anticipatory smooth pursuit and perceptual adaptation. *Journal of Vision*, *15*(2), 16–16. https://doi.org/10.1167/15.2.16

Montagnini, A., Souto, D., & Masson, G. (2010). Anticipatory eye-movements under uncertainty: A window onto the internal representation of a visuomotor prior. *Journal of Vision*, *10*(7), 554–554. https://doi.org/10.1167/10.7.554

Orban De Xivry, J. J., Missal, M., & Lefevre, P. (2008). A dynamic representation of target motion drives predictive smooth pursuit during target blanking. *Journal of Vision*, *8*(15), 6–6. https://doi.org/10.1167/8.15.6

Orban De Xivry, J.-J., Coppe, S., Blohm, G., & Lefèvre, P. (2013). Kalman Filtering Naturally Accounts for Visually Guided and Predictive Smooth Pursuit Dynamics. *The Journal of Neuroscience*, *33*(44), 17301–17313. https://doi.org/10.1523/JNEUROSCI.2321-13.2013

Orban De Xivry, J.-J., & Lefèvre, P. (2007). Saccades and pursuit: Two outcomes of a single sensorimotor process: Saccades and smooth pursuit eye movements. *The Journal of Physiology*, *584*(1), 11–23. https://doi.org/10.1113/jphysiol.2007.139881

Pasturel, C., Montagnini, A., & Perrinet, L. U. (2020). Humans adapt their anticipatory eye movements to the volatility of visual motion properties. *PLOS Computational Biology*, *16*(4), e1007438. https://doi.org/10.1371/journal.pcbi.1007438

Pasturel, C., Montagnini, A., & Perrinet, L. U. (2018). ANEMO: Quantitative tools for the ANalysis of Eye MOvements. *Grenoble Workshop on Models and Analysis of Eye Movements, Grenoble, France*. https://laurentperrinet.github.io/publication/pasturel-18-anemo

Price, N. S. C., Ono, S., Mustari, M. J., & Ibbotson, M. R. (2005). Comparing Acceleration and Speed Tuning in Macaque MT: Physiology and Modeling. *Journal of Neurophysiology*, *94*(5), 3451–3464. https://doi.org/10.1152/jn.00564.2005

Robinson, D. A. (1963). A Method of Measuring Eye Movemnent Using a Scieral Search Coil in a Magnetic Field. *IEEE Transactions on Bio-Medical Electronics*, *10*(4),

137–145. https://doi.org/10.1109/TBMEL.1963.4322822

Rottach, K. G., Zivotofsky, A. Z., Das, V. E., Averbuch-Heller, L., Discenna, A. O., Poonyathalang, A., & Leigh, R. J. (1996). Comparison of Horizontal, Vertical and Diagonal Smooth Pursuit Eye Movements in Normal Human Subjects. *Vision Research*, *36*(14), 2189–2195. https://doi.org/10.1016/0042-6989(95)00302-9

Santos, E. M., & Kowler, E. (2017). Anticipatory smooth pursuit eye movements evoked by probabilistic cues. *Journal of Vision*, *17*(13), 1–16. https://doi.org/10.1167/17.13.13

Schlack, A., Krekelberg, B., & Albright, T. D. (2007). Recent History of Stimulus Speeds Affects the Speed Tuning of Neurons in Area MT. *The Journal of Neuroscience*, *27*(41), 11009–11018. https://doi.org/10.1523/JNEUROSCI.3165-07.2007

Schmerler, J. (1976). The Visual Perception of Accelerated Motion. *Perception*, *5*(2), 167–185. https://doi.org/10.1068/p050167

Souto, D., Montagnini, A., & Masson, G. S. (2008). Scaling of anticipatory smooth pursuit eye movements with target speed probability. *Journal of Vision*, *8*(6), 665–665. https://doi.org/10.1167/8.6.665

Takeichi, N., Fukushima, J., Kurkin, S., Yamanobe, T., Shinmei, Y., & Fukushima, K. (2003). Directional asymmetry in smooth ocular tracking in the presence of visual background in young and adult primates. *Experimental Brain Research*, *149*(3), 380–390. https://doi.org/10.1007/s00221-002-1367-3

Tychsen, L., & Lisberger, S. G. (1986). Visual motion processing for the initiation of smooth-pursuit eye movements in humans. *Journal of Neurophysiology*, *56*(4), 953–968. https://doi.org/10.1152/jn.1986.56.4.953

Voeten, C. (2020). *buildmer: Stepwise elimination and term reordering for mixed-effects regression* [R].

Watamaniuk, S. N. J., & Heinen, S. J. (2003). Perceptual and oculomotor evidence of limitations on processing accelerating motion. *Journal of Vision*, *3*(11), 5. https://doi.org/10.1167/3.11.5

Werkhoven, P., Snippe, H. P., & Alexander, T. (1992). Visual processing of optic acceleration. *Vision Research*, *32*(12), 2313–2329. https://doi.org/10.1016/0042-6989(92)90095-Z

Zago, M., Iosa, M., Maffei, V., & Lacquaniti, F. (2010). Extrapolation of vertical target motion through a brief visual occlusion. *Experimental Brain Research*, *201*(3), 365–384. https://doi.org/10.1007/s00221-009-2041-9

Supplementary material

Final models for the LMM analysis

Exp 2A, constant speed probability-mixtures:

$$(6)\ aSPon \sim 1 + P(V33) + axis + (1 + P(V33) + axis \mid participant)$$

$$(7)\ aSPv \sim 1 + P(V33) + axis + (1 + P(V33) + axis \mid participant)$$

$$(8)\ SPlat \sim 1 + P(V33) * axis + P(V33) * Tk + (1 + P(V33) + axis + Tk \mid participant)$$

$$(9)\ SPacc \sim 1 + P(V33) * axis + P(V33) * Tk + axis * Tk + (1 + P(V33) + axis + Tk \mid participant)$$

Exp 2A-B, time-varying target kinematics probability-mixtures:

$$(10)\ aSPon \sim 1 + P(Vdec) + axis + (1 + P(Vdec) + axis \mid participant)$$

$$(11)\ aSPv \sim 1 + P(Vdec) + axis + (1 + P(Vdec) + axis \mid participant)$$

$$(12)\ SPlat \sim 1 + P(Vdec) * axis + P(Vdec) * Tk + (1 + P(Vdec) + axis + Tk \mid participant)$$

$$(13)\ SPacc \sim 1 + P(Vdec) * axis + Tk + (1 + P(Vdec) + axis + Tk \mid participant)$$

Exp 2A-B, comparison between target kinematics:

$$(14)\ aSPon \sim 1 + Tk + axis + (1 + axis \mid participant)$$

$$(15)\ aSPv \sim 1 + Tk * axis + Tk * exp + axis * exp + (1 + Tk + axis \mid participant)$$

$$(16) \quad SPlat \sim 1 + Tk * axis + Tk * exp + (1 + Tk + axis \mid participant)$$

$$(17) \quad SPacc \sim 1 + Tk * axis * exp + (1 + axis \mid participant)$$

LMM analysis - tables

Exp 1 - Anticipatory Parameters

	Dependent variable:	
	aSPon	aSPv
P(HS)	-15.90*** (-20.81, -10.99)	3.14*** (2.87, 3.41)
	t = -6.35	t = 22.80
Constant	-85.83*** (-100.04, -71.61)	2.55*** (2.01, 3.08)
	t = -11.83	t = 9.32
Random Effects		
Groups	3	3
sd(Constant)	14.92	0.57
sd(P(HS))	0.00	0.22
Note:	*p<0.05; **p<0.01; ***p<0.001	

Exp 2A, constant target speed - Anticipatory Parameters

	Dependent variable:	
	aSPon	aSPv
Axis[y]	0.02 (-10.34, 10.39)	-0.84*** (-1.32, -0.35)
	t = 0.004	t = -3.40
P(V33)	5.52 (-6.18, 17.22)	2.61*** (1.42, 3.79)
	t = 0.92	t = 4.31
Constant	-115.61*** (-128.62, -102.59)	2.45*** (1.58, 3.32)
	t = -17.41	t = 5.50
Random Effects		
Groups	13	13
sd(Constant)	21.37	1.63

sd(Axis)	15.68	0.86
sd(P(v33))	13.55	2.21
Note:		*p<0.05; **p<0.01; ***p<0.001

Exp 2A-B, accelerating target kinematics - Anticipatory Parameters

	Dependent variable:	
	aSPon	aSPv
Axis[y]	6.75 (-0.15, 13.66)	-0.61** (-1.04, -0.18)
	t = 1.92	t = -2.80
P(Vdec)	9.13* (0.35, 17.91)	2.25*** (1.53, 2.97)
	t = 2.04	t = 6.13
Constant	-123.73*** (-136.28, -111.18)	2.96*** (2.26, 3.65)
	t = -19.32	t = 8.35
Random Effects		
Groups	16	16
sd(Constant)	24.12	1.43
sd(Axis)	10.40	0.85
sd(P(Vdec))	9.79	1.43
Note:		*p<0.05; **p<0.01; ***p<0.001

Exp 2A-B, fully predictable target kinematics - Anticipatory Parameters

V11 as level 0

	Dependent variable:	
	aSPon	aSPv
V22	2.01 (-3.65, 7.67)	1.67*** (0.88, 2.45)
	t = 0.70	t = 4.18
V33	4.05 (-1.52, 9.63)	2.45*** (1.61, 3.29)
	t = 1.42	t = 5.73
Vacc	-7.82** (-13.60, -2.03)	0.38 (-0.27, 1.03)
	t = -2.65	t = 1.14
Vdec	-1.61 (-7.22, 4.01)	2.16*** (1.43, 2.89)
	t = -0.56	t = 5.77
Axis[y]	4.60 (-1.36, 10.56)	-0.35 (-0.82, 0.12)

	t = 1.51	t = -1.48
Experiment [constant time]		0.73*** (0.34, 1.13)
		t = 3.61
Axis:Experiment		-0.35* (-0.67, -0.02)
		t = -2.11
Constant	-119.31*** (-130.99, -107.63)	2.05*** (1.47, 2.63)
	t = -20.02	t = 6.94
Random Effects		
Groups	16	16
sd(Constant)	22.17	1.16
sd(Axis)	8.26	0.88
sd(V22)	NaN	1.56
sd(V33)	NaN	1.69
sd(Vacc)	NaN	1.27
sd(Vdec)	NaN	1.45
Note:		*p<0.05; **p<0.01; ***p<0.001

Exp 2A-B, fully predictable target kinematics - Anticipatory Parameters

V22 as level 0

	Dependent variable:	
	aSPon	aSPv
V11	-2.01 (-7.67, 3.65)	-1.67*** (-2.45, -0.88)
	t = -0.70	t = -4.18
V33	2.04 (-3.28, 7.36)	0.78 (-0.22, 1.79)
	t = 0.75	t = 1.53
Vacc	-9.83*** (-15.37, -4.29)	-1.29* (-2.34, -0.24)
	t = -3.48	t = -2.40
Vdec	-3.62 (-8.97, 1.73)	0.49 (-0.11, 1.09)
	t = -1.33	t = 1.61
Axis[y]	4.60 (-1.36, 10.56)	-0.58* (-1.05, -0.12)
	t = 1.51	t = -2.45
Experiment [constant time]		0.50* (0.11, 0.89)
		t = 2.53
Axis:Experiment		-0.35* (-0.67, -0.02)

		t = -2.11
Constant	-117.30*** (-128.85, -105.74)	3.72*** (2.97, 4.47)
	t = -19.90	t = 9.73
Random Effects		
Groups	16	16
sd(Constant)	22.17	1.64
sd(Axis)	8.26	0.88
sd(V22)	NaN	1.69
sd(V33)	NaN	2.06
sd(Vacc)	NaN	1.71
sd(Vdec)	NaN	1.48
Note:		*p<0.05; **p<0.01; ***p<0.001

Exp 2A-B, fully predictable target kinematics - Anticipatory Parameters

V33 as level 0

	Dependent variable:	
	aSPon	aSPv
V11	-4.05 (-9.63, 1.52)	-2.45*** (-3.29, -1.61)
	t = -1.42	t = -5.73
V22	-2.04 (-7.36, 3.28)	-0.78 (-1.79, 0.22)
	t = -0.75	t = -1.53
Vacc	-11.87*** (-17.33, -6.41)	-2.07*** (-2.92, -1.23)
	t = -4.26	t = -4.80
Vdec	-5.66* (-10.93, -0.39)	-0.29 (-1.04, 0.45)
	t = -2.11	t = -0.77
Axis[y]	4.60 (-1.36, 10.56)	-0.46 (-0.92, 0.01)
	t = 1.51	t = -1.92
Experiment [constant time]		0.50* (0.10, 0.90)
		t = 2.47
Axis:Experiment		-0.35* (-0.67, -0.02)
		t = -2.11
Constant	-115.25*** (-126.77, -103.74)	4.51*** (3.71, 5.30)
	t = -19.62	t = 11.06
Random Effects		

Groups	16	16
sd(Constant)	22.17	1.64
sd(Axis)	8.26	0.88
sd(V22)	NaN	1.69
sd(V33)	NaN	2.06
sd(Vacc)	NaN	1.71
sd(Vdec)	NaN	1.48

Note: $^{*}p<0.05$; $^{**}p<0.01$; $^{***}p<0.001$

Exp 2A-B, fully predictable target kinematics - Anticipatory Parameters

Vdec as level 0

	Dependent variable:	
	aSPon	aSPv
V11	1.61 (-4.01, 7.22)	-2.16*** (-2.89, -1.43)
	t = 0.56	t = -5.77
V22	3.62 (-1.73, 8.97)	-0.49 (-1.09, 0.11)
	t = 1.33	t = -1.61
V33	5.66* (0.39, 10.93)	0.29 (-0.45, 1.04)
	t = 2.11	t = 0.77
Vacc	-6.21* (-11.70, -0.72)	-1.78*** (-2.70, -0.86)
	t = -2.22	t = -3.80
Axis[y]	4.60 (-1.36, 10.56)	-0.73** (-1.19, -0.26)
	t = 1.51	t = -3.06
Experiment [constant time]		0.20 (-0.18, 0.58)
		t = 1.02
Axis:Experiment		-0.35* (-0.67, -0.02)
		t = -2.11
Constant	-120.91*** (-132.45, -109.38)	4.21*** (3.42, 5.00)
	t = -20.55	t = 10.47
Random Effects		
Groups	16	16
sd(Constant)	22.17	1.62
sd(Axis)	8.26	0.88

sd(V22)	NaN	1.45
sd(V33)	NaN	1.16
sd(Vacc)	NaN	1.48
sd(Vdec)	NaN	1.86
Note:		$^{*}p<0.05$; $^{**}p<0.01$; $^{***}p<0.001$

Exp 1 - Visually Guided Parameters

	Dependent variable:	
	SPlat	SPacc
P(HS)	1.84 (-1.10, 4.78)	31.94*** (23.22, 40.66)
	t = 1.23	t = 7.18
TargetVelocity [LS]	4.87*** (2.22, 7.52)	-45.38*** (-55.56, -35.20)
	t = 3.60	t = -8.74
P(HS):TargetVelocity	-1.63 (-4.94, 1.68)	-55.32*** (-63.74, -46.89)
	t = -0.97	t = -12.87
Constant	130.50*** (128.52, 132.49)	91.54*** (78.85, 104.23)
	t = 128.80	t = 14.14
Random Effects		
Groups	3	3
sd(Constant)	0.74	12.76
sd(P(HS))	1.82	6.83
sd(Target Velocity)	1.79	9.37
Note:		$^{*}p<0.05$; $^{**}p<0.01$; $^{***}p<0.001$

Exp 2A, constant target speed - Visually Guided Parameters

	Dependent variable:	
	SPlat	SPacc
Target Velocity [V11]	-16.15*** (-20.24, -12.07)	-36.91*** (-48.63, -25.19)
	t = -7.76	t = -6.17
P(V33)	-19.79*** (-25.49, -14.09)	8.25 (-0.29, 16.78)
	t = -6.81	t = 1.89
Axis[y]	0.01 (-3.00, 3.02)	17.57*** (8.58, 26.57)
	t = 0.01	t = 3.83

P(V33):Target Velocity	20.32*** (15.01, 25.63)	14.30** (4.21, 24.38)
	t = 7.50	t = 2.78
P(V33):Axis	5.41** (1.30, 9.51)	-16.80*** (-26.79, -6.80)
	t = 2.58	t = -3.29
Target Velocity:Axis		-11.11*** (-17.26, -4.96)
		t = -3.54
Constant	118.64*** (113.05, 124.22)	73.90*** (62.54, 85.25)
	t = 41.65	t = 12.75
Random Effects		
Groups	13	13
sd(Constant)	8.31	17.50
sd(P(V33))	6.28	NaN
sd(Target Velocity)	4.24	18.05
sd(Axis)	2.69	8.21
Note:		*p<0.05; **p<0.01; ***p<0.001

Exp 2A-B, accelerating target kinematics - Visually Guided Parameters

	Dependent variable:	
	SPlat	SPacc
Axis[y]	-1.01 (-3.67, 1.64)	2.48 (-8.26, 13.22)
	t = -0.75	t = 0.45
TargetVelocity [Vacc]	-7.20*** (-10.49, -3.90)	-33.71*** (-41.69, -25.74)
	t = -4.28	t = -8.29
P(Vdec)	-9.06*** (-13.75, -4.37)	-3.74 (-11.33, 3.85)
	t = -3.79	t = -0.97
P(Vdec):TargetVelocity	12.07*** (7.67, 16.47)	
	t = 5.38	
P(Vdec):Axis	5.38** (1.91, 8.86)	9.33** (2.90, 15.76)
	t = 3.03	t = 2.84
Constant	111.06*** (107.13, 114.98)	84.17*** (78.22, 90.13)
	t = 55.46	t = 27.71
Random Effects		
Groups	16	16
sd(Constant)	5.79	8.54

sd(Target Velocity)	3.94	15.43
sd(P(Vdec))	5.74	9.56
sd(Axis)	3.12	20.82
Note:		$^{*}p<0.05$; $^{**}p<0.01$; $^{***}p<0.001$

Exp 2A-B, fully predictable target kinematics - Visually Guided Parameters

V11 as level 0

	Dependent variable:	
	SPlat	SPacc
V22	2.56 (-1.58, 6.71)	25.75*** (22.03, 29.48)
	t = 1.21	t = 13.56
V33	-3.45 (-7.16, 0.26)	47.05*** (43.33, 50.77)
	t = -1.82	t = 24.81
Vacc	4.02* (0.30, 7.74)	12.44*** (8.70, 16.18)
	t = 2.12	t = 6.52
Vdec	0.42 (-3.81, 4.65)	39.49*** (35.78, 43.20)
	t = 0.19	t = 20.86
Experiment [constant time]	-0.46 (-4.07, 3.16)	0.12 (-5.96, 6.20)
	t = -0.25	t = 0.04
Axis[y]	1.59 (-0.96, 4.15)	2.91 (-2.81, 8.63)
	t = 1.22	t = 1.00
Axis:Experiment		-7.22 (-15.73, 1.28)
		t = -1.66
Constant	102.41*** (99.16, 105.66)	39.91*** (35.13, 44.69)
	t = 61.80	t = 16.37
Random Effects		
Groups	16	16
sd(Constant)	5.44	7.94
sd(V22)	6.57	NaN
sd(V33)	5.46	NaN
sd(Vacc)	5.39	NaN
sd(Vdec)	6.81	NaN
sd(Axis)	2.79	8.33
Note:		$^{*}p<0.05$; $^{**}p<0.01$; $^{***}p<0.001$

Exp 2A-B, fully predictable target kinematics - Visually Guided Parameters

V22 as level 0

	Dependent variable:	
	SPlat	SPacc
V11	-2.56 (-6.71, 1.58)	-25.75*** (-29.48, -22.03)
	t = -1.21	t = -13.56
V33	-6.01** (-10.09, -1.93)	21.30*** (17.67, 24.93)
	t = -2.89	t = 11.50
Vacc	1.46 (-2.40, 5.32)	-13.31*** (-16.96, -9.66)
	t = 0.74	t = -7.14
Vdec	-2.14 (-6.78, 2.49)	13.74*** (10.12, 17.36)
	t = -0.91	t = 7.43
Experiment [constant time]	1.86 (-1.96, 5.68)	4.25 (-1.70, 10.20)
	t = 0.95	t = 1.40
Axis[y]	1.00 (-1.50, 3.49)	5.49 (-0.11, 11.10)
	t = 0.78	t = 1.92
Axis:Experiment		-2.65 (-10.98, 5.67)
		t = -0.62
Constant	104.97*** (100.56, 109.39)	65.67*** (60.96, 70.38)
	t = 46.59	t = 27.31
Random Effects		
Groups	16	16
sd(Constant)	6.22	7.94
sd(V22)	5.39	NaN
sd(V33)	5.92	NaN
sd(Vacc)	6.15	NaN
sd(Vdec)	9.29	NaN
sd(Axis)	2.79	8.33
Note:		*p<0.05; **p<0.01; ***p<0.001

Exp 2A-B, fully predictable target kinematics - Visually Guided Parameters

V33 as level 0

	Dependent variable:

	SPlat	SPacc
V11	3.45 (-0.26, 7.16)	-47.05*** (-50.77, -43.33)
	t = 1.82	t = -24.81
V22	6.01** (1.93, 10.09)	-21.30*** (-24.93, -17.67)
	t = 2.89	t = -11.50
Vacc	7.47*** (3.56, 11.38)	-34.61*** (-38.25, -30.96)
	t = 3.75	t = -18.59
Vdec	3.87* (0.11, 7.63)	-7.56*** (-11.17, -3.94)
	t = 2.02	t = -4.10
Experiment [constant time]	1.70 (-1.84, 5.24)	6.73* (0.80, 12.65)
	t = 0.94	t = 2.22
Axis[y]	5.36*** (2.87, 7.84)	-5.56 (-11.16, 0.04)
	t = 4.22	t = -1.95
Axis:Experiment		0.24 (-8.05, 8.53)
		t = 0.06
Constant	98.96*** (94.91, 103.01)	86.96*** (82.26, 91.67)
	t = 47.91	t = 36.20
Random Effects		
Groups	16	16
sd(Constant)	6.22	7.94
sd(V22)	5.39	NaN
sd(V33)	5.92	NaN
sd(Vacc)	6.15	NaN
sd(Vdec)	9.29	NaN
sd(Axis)	2.79	8.33

Note: *p<0.05; **p<0.01; ***p<0.001

Exp 2A-B, fully predictable target kinematics - Visually Guided Parameters

Vacc as level 0

	Dependent variable:	
	SPlat	SPacc
V11	-4.02* (-7.74, -0.30)	-12.44*** (-16.18, -8.70)
	t = -2.12	t = -6.52
V22	-1.46 (-5.32, 2.40)	13.31*** (9.66, 16.96)

	t = -0.74	t = 7.14
V33	-7.47*** (-11.37, -3.56)	34.61*** (30.96, 38.25)
	t = -3.75	t = 18.59
Vdec	-3.60 (-8.81, 1.61)	27.05*** (23.41, 30.69)
	t = -1.35	t = 14.56
Experiment [constant time]	0.94 (-2.64, 4.53)	0.76 (-5.19, 6.72)
	t = 0.52	t = 0.25
Axis[y]	1.55 (-0.96, 4.05)	4.65 (-0.98, 10.28)
	t = 1.21	t = 1.62
Axis:Experiment		-3.85 (-12.18, 4.48)
		t = -0.91
Constant	106.43*** (102.90, 109.95)	52.36*** (47.63, 57.08)
	t = 59.17	t = 21.70
Random Effects		
Groups	16	16
sd(Constant)	6.22	7.94
sd(V22)	5.39	NaN
sd(V33)	5.92	NaN
sd(Vacc)	6.15	NaN
sd(Vdec)	9.29	NaN
sd(Axis)	2.79	8.33
Note:		*p<0.05; **p<0.01; ***p<0.001

Exp 2A-B, fully predictable target kinematics - Visually Guided Parameters

Vdec as level 0

	Dependent variable:	
	SPlat	SPacc
V11	-0.42 (-4.64, 3.81)	-39.49*** (-43.20, -35.78)
	t = -0.19	t = -20.86
V22	2.14 (-2.49, 6.78)	-13.74*** (-17.36, -10.12)
	t = 0.91	t = -7.43
V33	-3.87* (-7.63, -0.11)	7.56*** (3.94, 11.17)
	t = -2.02	t = 4.10
Vacc	3.60 (-1.61, 8.81)	-27.05*** (-30.69, -23.41)

	t = 1.35	t = -14.56
Experiment [constant time]	1.09 (-2.63, 4.82)	2.58 (-3.33, 8.48)
	t = 0.58	t = 0.85
Axis[y]	4.16** (1.68, 6.64)	6.11* (0.52, 11.71)
	t = 3.28	t = 2.14
Axis:Experiment		8.40* (0.14, 16.66)
		t = 1.99
Constant	102.83*** (98.71, 106.94)	79.41*** (74.70, 84.11)
	t = 48.99	t = 33.08
Random Effects		
Groups	16	16
sd(Constant)	6.22	7.94
sd(V22)	5.39	NaN
sd(V33)	5.92	NaN
sd(Vacc)	6.15	NaN
sd(Vdec)	9.29	NaN
sd(Axis)	2.79	8.33
Note:		*p<0.05; **p<0.01; ***p<0.001